The Pennsylvania State University

The Graduate School

Department of Materials Science and Engineering

ADSORPTION OF WATER ON SILICA AND SILICATE GLASSES

A Thesis in

Materials Science and Engineering

by

Betul Akkopru-Akgun

Submitted in Partial Fulfillment

of the Requirements

for the Degree of

Master of Science

May 2016

The thesis of Betul Akkopru Akgun was reviewed and approved* by the following:

Carlo G. Pantano
Distinguished Professor of Materials Science and Engineering
Thesis Adviser

Susan Trolier-McKinstry
Professor of Ceramic Science and Engineering

Seong Kim
Professor of Chemical Engineering

Suzanne Mohney
Professor of Materials Science and Engineering
Chair of the Intercollege Graduate Degree Program in Materials Science and Engineering

*Signatures are on file in the Graduate School

ABSTRACT

The aqueous surface chemistry of glasses has a significant effect on material properties, including chemical durability, mechanical strength and electrical conductivity. Thus, a fundamental understanding of water adsorption phenomena on glass surfaces is enormously important. This study examined adsorption phenomena on multicomponent glass surfaces by DRIFTs (Diffuse reflectance Fourier transform infrared spectroscopy) and TG-MS (Thermogravimetric mass spectroscopy). In particular, the effect of non-bridging oxygen and alkali/alkaline earth ions on the variation and concentration of surface adsorption sites, and eventually the degree of hydration, were examined on dry- and wet-ground multicomponent silicate glasses. For this purpose, commercial Ba-silicate, Ba-, Ca-, Mg-boroaluminosilicate, float glass, fused silica and fused quartz glasses have been used. The adsorbed water on the glass surface was distinguished from bulk water, trapped in interstices of silicate network, by D_2O exchange experiments. The variation in the glass surface composition as a function of the chemical composition and grinding media (wet or dry) was characterized by XPS (X-ray photoelectron spectroscopy). The effect of chemical structure on physically adsorbed water and chemisorbed water species on different multicomponent glasses were identified via adsorption/desorption experiments using in-situ DRIFTs.

The degree of hydration was found to vary depending on the concentration of Si-OH groups which is strongly dependent on the presence of (1) modifier ions or non-bridging oxygen, (2) glass intermediates (Al_2O_3 or B_2O_3) and (3) water already trapped in the bulk structure of the glass. For Ba-silicate and float glass with many non-bridging oxygen sites, the number of silanol groups (SiOH) and subsequent hydration rate is higher compared to fused silica and fused quartz. Moreover, $BaCO_3$ formation on the surface of Ba-silicate network also enhanced the degree of hydration. The number of water molecules on/in Ba-silicate glasses was found three times higher than pure silica counterparts. The presence of Al_2O_3 and B_2O_3 in modifier-containing silicate glasses decreases the number of NBO's due to their charge compensation of $[AlO_4]^-$ and $[BO_4]^-$ groups in the glass network structure. This limits the hydroxylation and subsequent hydration process. For this reason, the number of water adsorption sites in/on Ba-boraluminosilicate glasses was found considerably smaller than Ba-silicate. Besides the effect of chemical composition, the mechanical milling of glass powders in aqueous environments also promotes the degree of hydration. The effect of milling media is more predominant in Ba-silicate glasses with the high number of non-bridging oxygen.

TABLE of CONTENTS

LIST OF FIGURES

LIST OF TABLES

Chapter 1

INTRODUCTION

Understanding water adsorption phenomena on glass surfaces is enormously important for improvement of the properties of glass, which is crucial for development of next generation glasses. It is well known that interaction of water with glass surfaces may alter the surface chemistry of the glass and thus adversely affect the properties of the glass, including chemical durability, mechanical strength, fatigue life, refractive index and electrical conductivity. For example, adsorbed water, which is able to attack surface cracks, enhances the crack propagation and eventually reduces the glass strength [1]. Moreover, the attack of water on the glass surface may generate a hydrated layer, which makes the glass less durable under humid environmental conditions. The decrease in functional properties of glass surfaces may restrict their use in applications, which require high strength, stress-corrosion resistance, chemical durability and transparency. It is important, thus, to understand the chemical state and concentration of water-related species on glass surfaces.

The configuration of ions on silica and silicate glass surfaces is much different from that in the bulk. Unsaturated surface ions have an asymmetric distribution of attractive and repulsive forces and thus they can easily interact with atmospheric moisture to attain a state of minimal internal energy. Most of the silica surface terminates in either bridging oxygen (Si-O-Si) or silanol (Si-OH) groups. Furthermore, the atmospheric moisture may break strained Si-O-Si bonds to form additional surface hydroxyl groups in humid environments. This process is named chemisorption and necessitates high energy to overcome the energy barrier for formation of new chemical bonds. Silanol groups can be divided into three groups; (1) vicinal silanols where two OH groups are connected to the same Si atom, (2) geminal silanols, consists of two OH groups attached to different Si atoms and (3) free silanol groups where one OH group is connected to the Si atom. These silanol groups are preferential sites for further adsorption of water, named as physisorption where molecular water can connect to these silanol groups via H bonding. In contrast to chemisorption, physisorption does not require high energies because it just involves weak van der Waals forces instead of transfer or sharing of electrons. The concentration and distribution of these silanol groups determines the degree of hydration. Among all silanol types, vicinal OH groups have the highest affinity to interact with ambient moisture. The concentration of SiOH groups on amorphous silica was found 4.5/nm^2 [2]. The silanol groups can further interact with water and form multilayer adsorption of water molecules on the surface.

Physical adsorption of water (hydration) on multicomponent glass is quite different and more complex compared to silica because of the structural variation between them. For the pure silica, the available physorption sites on the surface are primarily silanol groups. For multicomponent glasses, on the other hand, additional active surface sites such as non-brigding oxygen or alkali ions on the surface enhance the adsorption of molecular water. The molecular water can react with non-bridging oxygen to form free modifier ions and H bonded silanol groups. The silanol groups have high reactivity to adsorb molecular water [2].

Moreover, multicomponent glasses allow a higher degree of hydration, (e.g. hydrated not only at the surface but also in the bulk (near-surface)) in contrast to pure silica surfaces where the formation of silanol groups is usually limited to a monolayer on the surface [3]. The effect of bulk structure on adsorption of water is higher in multicomponent glasses. The extent of water adsorption depth is related to the amount of alkali in glass [4]. When the alkali concentration is high, there is higher amount of non-bridging oxygen which are most likely react with adsorbed water (H_2O or/and H_3O^+) to form H-bonded Si-OH groups and free alkali ions. This leads to formation of a more open silicate network, which makes the attack of water on/in the glass structure easier. Additionally, free alkali ions near the surface can easily migrate to the surface and react with CO_2 to form carbonate [5-6]. The diffused alkali ions leave a space in the glass structure, enhancing the attack of water too. The concentration and type of available surface sites for adsorption of water is then influenced mainly by the chemical composition of underlying surface structure. Thus, understanding the role of non-bridging oxygen and alkali ions on the surface chemistry of glass is essential to determine water adsorption mechanisms at atomic level and degree of hydration on glass.

Fourier transform infrared spectroscopy (FTIR), nuclear magnetic resonance spectroscopy (NMR) and temperature programmed desorption spectroscopy (TPD) are the main techniques in the literature used to determine the type and concentration of water-related species as well as to investigate the hydration kinetics for silica and multicomponent glasses. The vast majority of these studies have been dedicated to hydration and hydroxylation of silica surface upon exposure to water vapor rather than multicomponent counterparts. Although there are a significant number of investigations on water dissolved in volcanic glasses during the melting process, they do not provide details about how the chemical composition of the bulk glass composition and structure influences the variation and concentration of surface adsorption sites. The number of studies on direct correlation of water adsorption sites with chemical changes of the bulk glass composition and structure is yet quite limited.

The main aim of this work is to investigate and define the surface adsorption sites on silica and silicate glass powders with distinct chemical composition by DRIFTs (Diffuse reflectance Fourier transform infrared spectroscopy) and TG-MS (Thermogravimetric mass spectroscopy). In particular, the effect of non-bridging oxygen and alkali/alkaline earth ions on the variation and concentration of surface adsorption sites and eventually the degree of hydration were examined

on dry- and wet-ground multicomponent silicate glasses. For this purpose, commercial Ba-silicate, Ba-, Ca-, Mg-boroaluminosilicate, float glass, fused silica and fused quartz have been used. The variation in the glass surface composition was measured by XPS (X-ray photoelectron spectroscopy). The effects of chemical composition on physically adsorbed water and chemisorbed water species on different multicomponent glasses were identified via in-situ desorption experiments in modified DRIFTs. The necessary temperatures for dehydration and dehydroxylation of glasses were determined. Moreover, the amount of H_2O adsorbed on different glass surfaces in the as-prepared condition and after rehydration under atmospheric moisture was determined by TG-MS.

This thesis includes 6 chapters. Chapter 2 presents a background literature review, including adsorption phenomena on glass surfaces, the surface chemistry of silica and multicomponent glass surface, and the effect of water adsorption on physical and chemical properties of glass surfaces. The differences between interaction of water with silica and multicomponent glass surfaces at the atomic level are discussed.

Chapter 3 presents the experimental procedure which includes grinding of the glass samples, their surface chemistry characterization in as-prepared condition and after heat treatment by XPS and DRIFTs and quantitative analysis of water-related species on/in glass by TG-MS.

In chapter 4, D_2O exchange experiments were used to differentiate surface and structural water for dry-ground silica and silicate glasses. The effect of milling on the surface composition was determined by XPS, while the chemical reactivity of glasses with different surface chemistries was investigated by DRIFTs and TG-MS. The correlation between concentration of non-bridging oxygen and reactivity of glass surface with water vapor was discussed based on the available literature. The degree of hydration for distinct multicomponent glasses was established by semi-quantitative TG-MS analysis and in-situ hydration experiments in DRIFTs.

Chapter 5 presents the effect of modifier ions, particle size and NBO on the variation and concentration of chemisorbed water species on glass surfaces, and the resultant degree of hydration for wet-ground multicomponent glasses. The effect of boron addition on surface structure of Ba-silicate glasses was investigated by XPS. The change in surface adsorption sites with addition of boron in Ba-silicate glasses was confirmed by in-situ DRIFT experiments. Moreover, the effect of grinding medium (wet and dry) on chemisorbed surface sites and resultant degree of hydration was discussed based on the variation on surface chemistry of wet and dry-ground multicomponent glasses.

Chapter 2

LITERATURE REVIEW

2.1 Adsorption Process on Glass Surfaces

2.1.1. Surface Forces Involved in Water Adsorption

The attraction and repulsion forces between ions control the structural arrangement of glass. Ions in glasses arranged themselves with opposite charge ions to minimize repulsion and maximize attraction forces. This kind of geometrical arrangment yields a minimum internal energy level. Attractive and repulsive forces between ions in glass structure are dependent on the size, polarizability and charge of the ions. The cations with small size and high positive charges, such as Si^{4+}, B^{3+}, are able to surround themselves with four oxygens, forming short-range order units link to create the glass network. On the other hand, low charge ions like Na^{+}, Ca^{2+} do not apply strong attraction forces to form their own coordination polyhedra, but instead, satisfy terminal charges on the three dimensional glass network [7].

The distribution of attractive and repulsive forces in glass networks differs from that of glass surface. In the bulk glass, a state of minimum internal energy is attained as a consequence of balance between attractive and repulsive forces, resulting from a symmetrical distribution of ions. The ions on the glass surface, on the other hand, differ from the bulk. Fracture of a glass leads to formation of incomplete coordination of surface cations which are subjected to an asymmetric distribution of attractive and repulsive forces. For this reason, the system is driven to lower its surface energy through (1) local rearrangments to shield excess surface charges or (2) adsorption of water molecules or other species from the surrounding atmosphere [7].

Si^{4+} surface ions with incomplete coordination increase the surface free energy of glass structure and act as the strongest adsorption sites. Alkali ions, on the other hand, are very polarizable and are able to redistribute their charge and also shield undercoordinated oxygens at the surface [7].

Any phonemona that can lead to a decline in surface free energy results in adsorption. Besides attraction and repulsion forces, electrostatic forces can also contribute to adsorbtion process when the adsorbate or adsorbant (surface) is polar. When the solid surface is polar, it generates dipoles in the adsorbing molecule [8].

2.1.2 Physical and Chemical Adsorption

Adsorption, an exothermic reaction, occurs through electrostatic attraction of water molecules (adsorbate) to a glass (adsorbent) surface. The adsorption of water molecules on the surface of glasses arises because surface ions of a glass are unsaturated and adsorption occurs to lower the surface free energy.

Adsorption of water can be classified as physical or chemical adsorption depending on the potential energy change. In physical adsorption, there are weak van der Waals forces between the water molecules and the glass surface. In contrast, chemisorption processes involve the formation of chemical bonds (covalent, ionic), i.e. a transfer or sharing of an electron, between the water molecules and glass surface. In general, chemisorption of water on glass requires exceeding a high activation barrier to break the strained Si-O-Si bonds, which is enhanced at higher temperatures. For the adsorption of water on E-glass, the required activation energy is about 3441.9 cal/mole [9].

In contrast to their crystal counterparts, glass surfaces have a wide distribution of possible energetically different chemisorptions sites, such as non-bridging oxygens, alkali cations, and siloxane linkages. Hydroxylation or chemisorption of water breaks –Si-O-Si- bonds and forms –Si-OH- groups. The physical adsorption of water preferentially occurs on these hydroxyl groups. Figure 2.1 schematically describes the physisorption and chemisorption of water on a glass surface [10].

The degree of interaction between glass surface and water is strongly dependent on the reactivity or/and energy of possible adsorption sites. Glass surfaces which have irregular atomic arrangment may have a wide distribution of surface sites for adsorption of water, in contrast to their crystal counterparts. The presence of energitically heterogenous surface sites on glass makes the adsorption/desorption spectra more complicated.

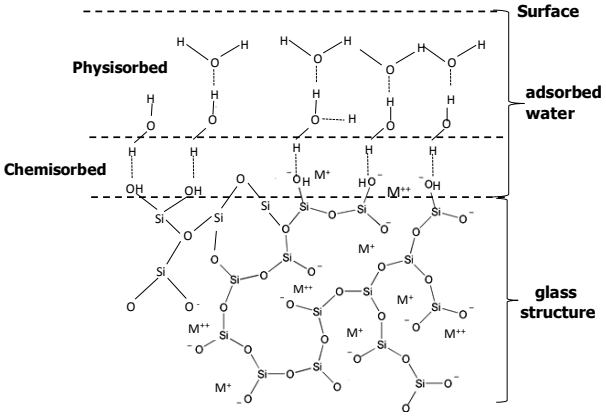

Figure 2.1 *Physisorption and chemisorpuon of water on glass surface [12]*

2.1.3 The Effect of Water on Physical and Chemical Properties of Glass

Silica-based glass surfaces consist of strained siloxane and silanol groups which have a high tendecy to react with water. The moleculer water can easily adsorb on the strong physisorption sites, followed by chemisorption process, which requires higher energy to break surface bonds. The attack of water eventually change the surface chemistry of glass surface and weakens the silicate network [11].

The structural change in/on the glass has a profound effect both on bulk and surface properties of the glasses. It has been shown that a trace amount of water incorporation into glass reduces the viscosity, glass transition temperature [3], refraction index, mechanical strength, fatigue resistance [12-13] and infrared transmittence [14] while it leads to an increase in the thermal expansion coefficient [14], and crystallization rate [15].

Similar to bulk water in glass, water adsorbed on the glass surface also has an influence on the physical and chemical properties of glass. Surface water may change, mechanical strength, surface tension (wetting property), infrared transmittence and electrical conductivity [83]. The presence of adsorbed water on glass surface greatly affects mechanical properties, including strength, fracture toughness and fatigue life of glass. The surface flaws present on glass are more prone to react with adsorbed water rather than siloxane groups (Si-O-Si). The water moves along the crack decreasing the bond strength at the crack tip. This promotes the propogation of surface cracks, leading to a decrease in fracture strength and enhancing the fatigue [1]. It has been found that the presence of a 100 nm long water adsorbed at the crack tip on fused silica glasses enhances the crack propagation [16].

Adsorbed water on glass surface also influences the electrical conductivity. It has been proposed that Si-OH groups or water molecules on the glass surface can dissociate to create protons which are mainly responsible for enhancement in the electrical conductivity. The extent of dissociation of charged particles was found strongly depend on surface concentration of adsorbed water on glass surface [17]. Surface conduction arising from protonic species becomes greater with an increase in concentration of water [17]. Moreover, free mobile surface cations can contribute to electrical conductivity if a leached layer forms during attack of water on the glass surface [18].

Another significant property which is influenced by water adsorption on glass surface is wetting. The adsorption of water on glass surfaces reduces the critical surface tension of wetting, leading to formation of hydrophilic surfaces. It has been demonstrated that adsorbed water on borosilicate glass and fused quartz makes the surfaces more hydrophilic by decreasing the critical surface tension of wetting [19].

Water on glass surface also changes the property of infrared absorption within the glass. The formation of H-bonded and isolated OH groups leads to the apperance of an IR band at 3500 and

3750 cm^{-1}. Adsorption of molecular water also leads to emergence of IR band at 3400 and 1627 cm^{-1} [20].

2.2 Surface Chemistry of Silica and Silicate Glasses

2.2.1 Silica

Silica, consisting of fully cross-linked SiO_4 tetrahedra, is a major component for most glasses. Thus, understanding the surface chemistry of silica is crucial to obtain deeper understanding of adsorption phenomena on silicate network of multicomponent silicate glasses.

In amorphous silica, surface silicon atoms have unsatisfied bonds. These bonds can react easily with atmospheric moisture to form saturated silanol groups. The surface of silica is consisted of siloxane group (≡Si-O-Si≡) or/and silanol groups (≡Si-OH). There are three distinct silanol configurations as shown in Figure 2.2: (1) isolated groups (or free silanols), where the surface Si atom connected to single free OH group on the surface it has a 3 bonds with O in the bulk, (2) vicinal silanols (or bridged silanols) involving two H bonded hydroxyl groups, attached to different Si atoms, and (3) geminal silanol consists of two single silanol groups connected to same Si atom. These silanol groups are preferential sites for interaction of the silica surface with species like CO_2, H_2O, N_2, CO as well as organics [21]. Silanols interact with molecular water through hydrogen bonding [22].

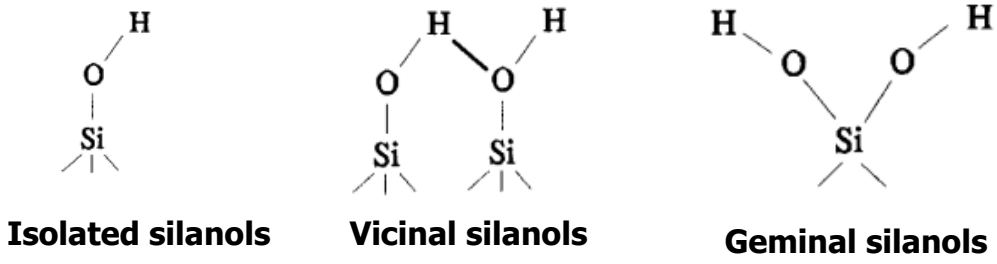

Figure 2.2 *Distinct silanol (Si-OH) groups on amorphous silica [2]*

The surface structure of amorphous silica is highly disordered; thus the arrangement of hydroxyl groups on the silica surface is irregular. The surface of silica is covered by isolated as well as vicinal OH groups. When the complete coverage of hydroxyl groups on silica surface is achieved, the surface is termed fully hydroxylated. The concentration of hydroxyl groups on amorphous silica surface was found 4.6 OH/nm^2 [2]. The concentration and configuration of silanols on silica surfaces determines the extent of physical adsorption of molecular water [23]. Among all silanol types, including isolated, germinal and vicinal groups, vicinal groups have more affinity or accessibility to interact with molecular water. Molecular water is physically adsorbed to the silica surface through hydrogen bonds with the vicinal silanol groups. The uptake of physically adsorbed water on a fully hydroxylated silica surface is called hydration. In a fully hydroxylated silica surface, a multilayer of adsorbed water is built up by increasing the partial

pressure. Figure 2.3 depicts the schematic representation of hydrated and hydroxylated silica surface. As shown in Figure 2.3, the surface silicon atoms, tetrahedrally coordinated to three other oxygen atoms complete their coordination number by attachment to the monovalent hydroxyl group rather than formation of strained siloxane groups. Physically adsorbed water molecules preferentially connect to these silanol groups through hydrogen bonding.

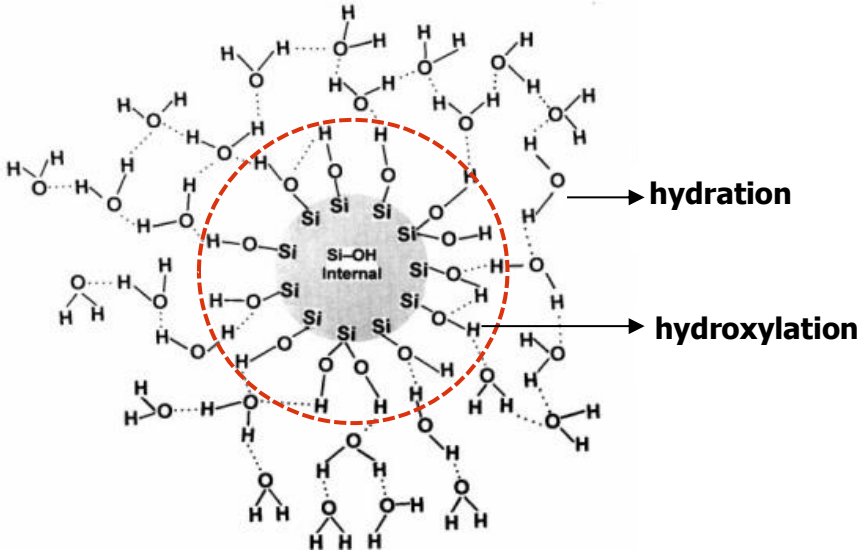

Figure 2.3 *Schematic representation of hydroxylated and hydrated silica surface [2]*

The adsorption of water on silica surfaces, consisting of the two basic steps; hydroxylation and hydration, has been studied extensively with infrared spectroscopy [21, 24-25]. The physically adsorbed water and all types of silanol groups on the silica surface lead to the appearance of distinct IR bands in the mid infrared region. The isolated and vicinal SiOHs give a sharp band located at 3747 cm^{-1} and a relatively broad band at 3660cm^{-1}, respectively. The physically adsorbed water also leads to emergence of a broad band centered at 3400 cm^{-1}.

Both physically and chemically adsorbed water can be removed from the silica surface with heat treatment. It has been found that silica dried in air at low temperatures (120-150°C) [26] or upon vacuum evacuation at room temperature, lost all physically adsorbed water. However, if the silica contains some porosity, adsorbed water can be retained in micropores up to 180-200°C. In the dehydration process, multiple layers of physically adsorbed water are removed in the temperature range of 25-150°C while the SiO_2 surface remains in a state of maximum hydroxylation. The hydration process is reversible upon the reintroduction of excess water [2]. On the other hand, removal of chemisorbed water is more difficult. Temperatures of 500°C and higher are required for dehydroxylation of silica surfaces [25]. From 200 to 400°C, the concentration of vicinal hydroxyl groups decreases, and finally all hydrogen bonded vicinal OH^- groups condense to produce a siloxane linkage (≡Si-O-Si≡) and molecular water [21-24]. Most of the isolated and germinal OH^- groups still remain on the silica surface after heat treatment at 400°C. Further heating at 800°C leads to removal of most of geminal and internal OH^- groups

while isolated single silanols remain still on the surface. Finally, isolated silanols are removed from the silica surface after heating above T_g (Glass transition temperature) [2].

The critical temperature for removal of silanols from the silica surface is strongly dependent on morphology, the surface area of the silica as well as the pore size and the presence of impurities on the silica surface. For instance, the presence of K^+ ions on silica surface lowers the dehydroxylation temperature by 100-200°C [25]. Moreover, for smaller particle sizes, the small radius of curvature leads to an increase in the intersilanol distances and thus deyhdroxylation is enhanced. Similar to the particle size effect, the decrease in pore size leads to slower dehydroylation behavior. Because smaller pores have a more negative radius of curvature, the distance between Si-OH groups decreases and thus, the dehydroxylation of SiO_2 surface becomes more easily [25].

The isolated silanol groups are the surface sites which determine the chemical reactivity of SiO_2 surface. Thus, estimation of this Si-OH concentration is crucial. It can be measured by infrared spectroscopy (IR) [26], nuclear magnetic resonance spectroscopy (NMR) [27] or thermogravimetric spectroscopy (TGA) [28].

Infrared Spectroscopy is the most commonly used technique which provides both qualitative and quantitative information on different types of Si-OH groups. Because distinguishing the surface silanol groups and physically adsorbed water in the mid-infrared region is difficult, the near-infrared region is mostly used for determination of the concentration of different water species (physically adsorbed water, isolated free silanols and hydrogen bonded silanol groups with IR band positions centered at 5235, 4425 and 4505 cm^{-1}, respectively). Additionally, the molar adsorption coefficients were found

0.89 ± 0.03 and 0.35 ± 0.02 for 4425 and 4505 cm^{-1} IR bands; these were attributed to hydrogen-bonded and free silanol groups, respectively [26].

Another method to determine the hydroxyl concentration is solid-state NMR spectroscopy. The relative amounts of silanol groups can be defined through using ^{29}Si CPMAS NMR (Si cross polarization magic-angle spinning) and silylation. However, NMR is a bulk method and its quantitative result also includes bulk OH groups in SiO_2 [27].

Additionaly, TGMS (Thermogravimetric Mass Spectroscopy) or TGA (Thermogravimetric Analysis) is often used to estimate the concentration of Si-OH groups on SiO_2 surfaces. Because there is no way to distinguish different water species with TGA, TGA is used together with either Infrared spectroscopy [28] or DTA (Differential Thermal Analysis) Spectroscopy to estimate the surface silanol concentration [27].

Distinguishing the Si-OH groups on silica surfaces from other type of water species like physically adsorbed water or bulk (internal) water is very important to calculate the silanol density on the surface. Some water molecules might be strongly held together at the temperature of dehydration (50-190°C) or some silonals may condense at the temperature of hydration (50-190°C) [28]. One of the common methods to differentiate types of water molecules is called deuteration. In this process, D_2O, which is known as heavy water, is contacted to a SiO_2 surface which is partially or fully dehydroxylated through pretreatment in the range of 150-300°C. Then, the produced vapour is analyzed through mass spectroscopy to determine the silanol concentration exchanged with D_2O [28-29]. Deuteration of fully hydroxylated silica does not result in full exchange of hydroxyl groups because internal or structural Si-OH groups are not accessible for D_2O exchange reaction [30]. For a fully hydroxylated SiO_2 surface, the concentration of silanol was found as 4.6±0.5 OH/nm^2 [2]. In addition, other hydrogen sequestering agents ($ZnMe_2$, BCl_3, $TiCl_4$, $AlMe_3$, $GaMe_3$, Bet_3 and $(SiMe_3)_2NH$) with distinct steric dimensions, were used to study silanol groups on SiO_2 surface with Infrared Spectroscopy. It was shown that the number of accessible H-bonded OH groups is strongly dependent on the reactant's size and shape. Smaller reactants have a great ability to access the H-bonded silanols compared to larger ones [31].

Another approach to distinguish water species on the SiO_2 surface is the Karl Fisher Titration Reagent Method, sensitive even to small amounts of water. Karl Fisher Titration agents react with physically adsorbed water but not silanol groups on the SiO_2 surface. Thus, when the total concentration of silanol and physically adsorbed water is known, the amount of physically and chemically adsorbed water can be estimated separately. Kellum and Smith established the concentration of the adsorbed water in the presence of silanol groups using Karl Fisher Titration Reagent method. For this method, silica particles were added into a solution of Karl Fisher reagent and Lorol5-pyridine-alcohol diluent in the titration cell, consisting of platinum electrodes and biamperometric apparatus. Then 200 mV is applied to electrodes. In general, high molecular weight alcohol is used to prevent reaction between silanol and alcohol groups. The increase in the current was compensated with addition of Karl Fisher titration agent-methanol mixture; the adsorbed water concentration can be determined by thermogravimetric analysis or/and azeotropic distillation methods [32].

Silanol condensation procedure can be used to determine the total concentration of hydroxyl groups in silica materials. In this method, boron trifluoride, acetic acid and pyridine were used as catalyst. Then, the Karl Fisher reagent-methanol mixture is introduced into system. The two-step attack of methanol on hydroxylated silica surface can occur,

$$\equiv SiO\text{-}Si\equiv + CH_3OH \longrightarrow \equiv SiOCH_3 + \equiv SiOH \qquad \text{Eq (2.1)}$$

$$\equiv SiOH + CH_3OH \longrightarrow \equiv SiOCH_3 + H_2O \text{ (in the excess of methanol)} \qquad \text{Eq (2.2)}$$

The total amount of water can be found using the following equation [33].

$$\%OH\ (total) = \frac{KFR\ (ml)(F_1)(C)(A)(100)}{sample\ weight} \quad \text{Eq (2.3)}$$

Where C= conversion factor for the condensation reaction 1.88, A= Aliquot factor, F_1= grams H_2O/ml KFR in methanol diluents (KFR= Karl-Fisher reagent)

$$\%OH\ (silanol) = \%\ OH\ (total) - \ \%\ OH\ (H_2O) \quad \text{Eq (2.4)}$$

$$\%OH\ (H_2\ O) = \frac{KFR\ (ml)(F_2)(C)(100)}{sample\ weight} \quad \text{Eq (2.5)}$$

Where F_2= grams H_2O/ml KFR in high molecular weight alcohol

2.2.2 Multicomponent (Silicate) Glasses

It is also a well known fact that water interacts with multicomponent glass surfaces through hydration and ion exchange processes [34]. Multicomponent glasses can hydrate not only at the surface but also in the bulk (near-surface) [3]. The formation of s ilanol groups on silica glass is usually limited to the outermost monolayer. Physical adsorption of water on multicomponent glasses, on the other hand, is quite different and more complex compared to pure silica [3]. In the case of pure silica, adsorption of water on silica is usually limited to weakly H bonded silanol sites present on the surface. In contrast, multicomponent glasses, containing alkali ions, have additional adsorption sites such as non-bridging oxygen (NBO) and modifier ions (Li, Na, K, Ca, Ba), where the alkali ions are able to adsorb molecular water. The adsorbed water may react with (NBO) to form free silanol and alkali ions. The reactions between water and these adsorption sites are shown in the equations below [23].

$\equiv Si^+ + H_2O \longrightarrow \equiv$ Si-OH + H^+ Eq (2.6)

$\equiv SiO^- + H_2O \longrightarrow \equiv$ Si-OH + OH^- Eq (2.7)

$\equiv$Si-O-Si$\equiv + H_2O \longrightarrow$ 2($\equiv$ Si-OH) Eq (2.8)

$\equiv Si^-OX + H_2O \longrightarrow \equiv$ Si-OH + XOH where X=Li, Na, K, Ca, Ba, Pb, etc. [23] Eq (2.9)

The extent of water adsorption depth is directly related to the amount of alkali in the glass [4]. When the alkali concentration is high, the adsorbed water reacts with the non-bridging oxygen to form free OH and alkali ions. Then, Si-O-Si bonds are further weakened due to reaction of Si-O-Si linkage with molecular water. Additionally, free alkali ions migrate to glass surface, leaving a hole in the glass network. This makes attack of more water on/in glass structure easier, and as a

result, a hydrated porous layer forms on the glass surface due to breakdown of siloxane bridges [23]. The alkali ions on glass surface can react with CO_2 to form Na-carbonate [6].

The porous layer forms as a result of reaction of SiO_2 network with molecular water [35]:

$$Si\text{-}O\text{-}Si + 3H_2O = SiOHOH_2 + H_2OHOSi \qquad \text{Eq (2.10)}$$

Formation of the surface hydrated layer, often named microporous gel, occurs if the alkali oxide content of glass is higher than 20%. Lower alkali containing glasses like soda-lime silica, borosilicate glasses do not form porous hydrated layers on the surface. For a given modifier, the reactivity of alkali silicate glasses is enhanced with increasing non-bridging oxygen content. However, for glasses with the same alkali ion content, the larger the ionic radius of the modifier ions, the more reactive the glass will be. Larger cations like K^+ leave behind larger voids after exchange reaction, which makes access of molecular water to the sub-surface of glass easier [36]. Additionally, the substitution of alkaline earth ions (RO) instead of (R_2O) always decreases the hydration rate up to some extent and the effect becomes larger in the order MgO < BaO < SrO CaO< PbO < ZnO in alkali containing silicate glasses [36].

The effect of alkali ions on hydration of glass surfaces can be explained through the polarizing power of atoms on the glass. O^{2-} ions are very polarizable. However, when oxygen atom is fully coordinated with two silicon ions, it becomes non-polarizable. On the other hand, non-bridging oxygens, formed through introduction of alkali ions into silicate glasses, are very polarizable and can easily form hydrogen bonding with silanol groups. The polarizing power of cations in silicate glass also has a strong effect on adsorbtion phenomena [37]. When the polarizing power of Si^{4+} increases, the chance of formation of hydrogen bonded silanol decreases since all the oxygens in the glass are rigid. However, as the concentration of alkali ions increases, the polarizing power of cations diminishes, leading to higher fraction of hydrogen bonded silanol groups. Near Infrared Spectroscopy results showed that there is a significant increase in the intensity of H bonded OH groups (4552 cm^{-1}), which are strongly bonded to non-bridging oxygen in silicate networks [37]. It is well known that molecular water preferentially tends to adsorb on these H-bonded OH groups. Thus increasing alkali ion concentration enhances possibility of hydration of the glass network.

It has been determined that the concentrations of H-bonded and isolated OH in hydrated glass increases till the total water concentration is 7 wt% H_2O. Any additional water higher than 7 wt% is associated to molecular water and H-bonded silanol groups. The concentration of water adsorbed increases with decreasing hydration temperature. Hydration of glass is improved with higher hydration temperature up to 350°C. The adsorbed water on glass surfaces can be divided into two groups; tightly bonded water (which is released in the 350-550°C region) and loosely bounded water (released afer heat treatment at about 200°C) [37]. The former consists of silanol

groups as well as monomeric molecular water, while the latter is referred to as loosely bonded monomeric molecular water.

Infrared Spectroscopy is the main technique to investigate the chemical state of water in/on silicate glasses upon exposure to water. To date many studies have been done to determine the type of water species in silicate glass to explain possible adsorption sites or/and mechanism for hydration of glass. But, in most studies up to now, hydration of bulk glass has been taken into account [36, 38-48]. Relatively fewer studies have been done on hydration of glass surfaces [35, 49-51].

In the mid IR region, the infrared spectra of silica or/and aluminosilicate glasses, which may contain very small amount of non-bridging oxygen (NBO), is mainly consisted of three absorption bands at (1) 3500 cm^{-1}, assigned to asymmetric OH stretching vibration, (2) 3400 cm^{-1}, attributed to molecular water and, (3) 1630 cm^{-1} associated with the fundamental bending mode of water molecule [39]. Additionally, internal OH groups in silicate glasses are represented by an absorption band at 3650 cm^{-1} [35]. Glasses with a significant amount of alkali ions, on the other hand, exhibit some additional absorption bands located at 2350 and 2850 cm^{-1}. The former represents the Si-O-H groups that form very strong hydrogen bonding with the non-bridging oxygen of isolated tetrahedron (Q_0) and the latter is attributed to the Si-O-H groups that form weak hydrogen bonding with the non-bridging oxygen of Q_2 (silicate tetrahedron linked to two other tetrahedrons by sharing two oxygen atoms) or Q_3 (silicate tetrahedron attached to three other tetrahedrons by sharing three oxygen atoms) tetrahedron [53]. The bands located at 2350 and 2800 cm^{-1} were also described as OH stretching modes of strongly bonded water molecule between two non-bridging and cation dipoles [54]. The presence of non-bridging oxygen on/near glass surface enhances the hydrogen bonded hydroxyl formation in the alkali silicate glasses. In addition, the infrared band at 1760 cm^{-1} appears for glass structure with a high concentration of alkali ions as a result of interaction of molecular water to the non-bridging oxygen site. During this interaction, water molecule forms very strong hydrogen bonding with O_2^- in the glass network [51]. The position of infrared bands related to possible water species on or near-surface are shown in Table 2.1.

It has been shown that the relative intensities of these infrared bands, i.e. the ratio of Si-OH band to H_2O, can be changed with composition or temperature. The intensity of the band at 3600 cm^{-1} associated with OH stretching of Si-OH groups, increases, while the intensity of bands located at 2350 and 2800 cm^{-1} due to OH stretching modes of a hydrogen bonded water molecule to non-bridging oxygen decreases with increasing temperature or the decrease in the size of alkali ion (in the order of K-Na-Li). The frequency of H-bonded hydroxyl groups is dependent on the chemical composition of glass. It has been observed that substitution of Al^{3+} for Si^{4+} in

Table 2.1 *The position of infrared bands related to possible water species on or near the glass surface*

Type of group	**Wavenumber (cm^{-1})**	**Refs**
Isolated SiOH	3750	[35]
Pairs of SiOH weakly H bonded	3590	[38, 39, 58]
Physically adsorbed water	3200, 3450	[58]
Internal hydroxyl groups	3650	[35]
Molecular water	1640	[53]
SiOH H-bonded to NBO	2350	[38-40]
SiOH H-bonded to NBO	2800	[38-40]

tetrahedrally coordinated structure decreases the fundamental OH stretch frequencies by 100 cm^{-1}. This occurs due to decrease in ionic potential of the bonded cation from Z/r(Si)~10 to Z/r(Al)~6 (where z is the formal charge and r is the ionic radius). Cations with Z/r>1 are able to polarize O atoms, extracting electron density from O-H bonds, leading to an increase in O-H distances and eventually lowering the OH frequencies. Substitution of B (Z/r~12) does not affect the frequency of OH vibration significantly. The strongest effect was observed at a higher ionic potential (Z/r(Si)~10 to Z/r(Li)~1.1) where cation strength is shared among four A-OH bonds [55]. The surface treatment of porous glass with boric acid resulted in appearance of an additional infrared band located at 3703 cm^{-1}, corresponding to surface B-OH groups.

Because Si-OH bands are located at the same region with molecular water (3400-3500 cm^{-1}), near IR measurements have been done to differentiate the type of water species on/in silicate glasses. The Si-OH combination stretch of hydroxyl groups bonded as Si-OH, Al-OH, has an additional band at 4520 cm^{-1} in the near IR region. Previous studies showed that the band at 4520 cm^{-1} disappeared when the total concentration in soda-lime-silica glass is greater than 5 wt%. The total OH concentration associated to this band was found 3 wt% in this glass [51]. The band at 5230 cm^{-1} in near IR region represents the OH stretching and HOH bending of molecular water [57]. There is an additional band at 7100cm^{-1}, representing the overtone of the fundamental OH stretch that is present both in hydroxyl and molecular water. The intensity of this band is enhanced with an increase in the amount of water in glass structure [58].

The type of water species in glass network can be also differentiated via NMR (Nuclear Magnetic Resonance) Spectroscopy. The MAS NMR spectra for hydrous sodium silicate consists of four resonance bands located at 3.2, 4.5, 4.7, 4.3 p.p.m. (Parts per million shift of the resonance line relative to TMS (tetramethylsilane) with an extensive spinning-side-band system and 12 p.p.m. with only two pairs of spinning side bands. The peaks at 4-5 p.p.m. are due to presence of molecular water in silicate glass [59]. The resonance band located at 3.2 p.p.m. is attributed to hydroxyl groups in glass structure. The proton resonance at higher frequencies (11-17 p.p.m.) indicates the presence of strong hydrogen bonding, formed as a result of interaction between Si-OH and O-Si [60]. It has been observed that hydration of sodium silicate resulted in a chemical shift of about 8 p.p.m. to the higher field in Si^{29} spectra due to shielding effect of water

molecules associated to SiO_4 tetrahedron. There is also an additional chemical shift about 2 p.p.m. in the position of NMR peak in ^{23}Na spectra after hydration of sodium silicate glass. This indicates that water molecule is associated with Na^+ in hydrated glass [47].

The concentration of molecular water as well as hydroxyl groups adsorbed in/on have been calculated by using Bouguer-Beer-Lambert Law: C=A/εL where A is the maximum height of an optical absorbance band or the area under the band; ε is the extinction coefficient for that band, i.e. the molar absorptivity ($lmol^{-1}cm^{-1}$) and L is the path length of the light through the host material. The most critical part in this equation is determination of molar absorptivity because attempts made to calculate molar absorptivity, produced widely scattered results [61]. The molar absorption coefficient is composition dependent and need to be calibrated to use for a particular composition of glass [61]. The absorption coefficient increases with increasing mole fraction of cations (Al^{3+}, Si^{4+}) in the glass composition. Previous studies have also shown that the absorption coefficient increases with increasing alkali concentration and the size of alkali ions. The concentration of adsorbed molecular water and OH groups emerged in DRIFT spectra (Diffuse reflectance infrared spectra can be estimated by using Kubelka-Munk theory.

$$F(R_\infty) = \frac{(1-R_\infty)}{2R_\infty} = \frac{K}{S} = \frac{2.303\varepsilon C}{S} \qquad \text{Eq (2.11)}$$

where $R_\infty$is the reflectance from a specimen of infinite thickness, K is the absorption coefficient, S is the scattering coefficient, ε is absorptivity and C is the concentration. Because the scattering coefficient is strongly dependent on particle size, refractive index, the linearity between $F(R_\infty)$ and concentration is rarely accomplished and this decreases the reliability of the quantitative analysis. In general, DRIFT spectra are normalized by using the same reference IR band for all samples [62]

The concentration of molecular water exhibits a strong dependence on total amount of water in/on glass. No molecular water is determined for the soda lime silica glass with 0.2 weight percent of total water [81]. When the total amount of water exceeds 0.5 weight percent, molecular water is detected and the amount of molecular water is related to the total water concentration in/on the glass. Hydroxyl species are main components at low hydration rates. The concentration of hydroxyl groups also increases with increasing total concentrations but the increase in hydroxyl groups is much smaller when the total amount of water is higher than 3 percent. The molecular water starts to release from glass during heat treatment higher than 200°C [38, 57]. At higher total water contents, the saturation level of OH concentration has been found as 2.2%wt for soda lime silica glass [63]. NMR is another technique widely used for determination of water concentration in glasses. Quantitative NMR results exhibit similarity with quantitative data obtained from Infrared Spectroscopy. It has been observed that the molecular water is dominant species at higher total water content and its concentration increases with further increase in total water concentrations [42, 64].

Chapter 3

MATERIALS and METHODS

3.1 Preparation of Glass Powders

In this study, commercial fused silica, fused quartz and multicomponent glasses with distinct chemical compositions were used to investigate water adsorption on glass surfaces. Most of the multicomponent glasses used here were provided by Schott Glass Company. These glasses are Ba-silicate ($BaO.2SiO_2$) and alkali free, i.e Ba-, Ca-, Mg-boroaluminosilicate glasses with a bulk composition of $12\%RO.15\%B_2O_3$. $9\%Al_2O_3.63\%SiO_2$, respectively. Additionally, commercial soda-lime silica glass (float glass; Asahi Glass Company) was used with a bulk chemical composition of 14% $Na_2O.9\%CaO.5\%MgO.72\%SiO_2$. Fused silica (Corning, 1980) and fused quartz were also used as reference materials.

3.1.1 Wet Grinding Process

A conventional wet milling technique was used to prepare are Ba-silicate and alkali free, i.e Ba-, Ca-, Mg-boroaluminosilicate glass samples. Typically, a mixture of water and zirconia balls was prepared in polytetrafluoethylene cup. Then, glass samples were dispersed homogenously in this mixture and ground at 2000 rpm for 2h. The resultant glass and water mixture is centrifuged to remove any larger glass particles. Finally, the centrifuged glass powders were dried to remove any remaining water. The particle size distribution of powders was measured using a particle size analyzer (Malvern Mastersizer). The final particle size of all glass powders was approximately 1.5 μm. Ba-boroaluminosilicate ($BaO.Al_2O_3.B_2O_3.SiO_2$) glass sample was further ground to obtain finer glass particles about 1, 0.7 and 0.4 μm using the wet milling technique.

3.1.2 Dry Grinding Process

Glass samples, i.e. Ba-silicate ($BaO.SiO_2$), Ba-boroaluminosilicate ($BaO.Al_2O_3.B_2O_3.SiO_2$), soda-lime-silica ($Na_2O.CaO.SiO_2$), Fused silica and fused quartz, were first crushed to millimeter-sized fragments by using Retsch Vibratory Disc Mill RS 200 at 1500 rpm for 30 sec. Then, the crushed glass samples were groundd by zirconia mortar and pestle and sieved to various size fractions such as 75, 45 and 20 μm. Glass powders were further ground by mortar and pestle for 3 days to obtain much finer particles (smaller than 10μm). The particle size distribution of the powder was determined by a Malvern Mastersizer. These fine glass powders AAszwere used for characterization of these powders as well as for adsorption experiments.

3.2 Characterization of Glass Powders

3.2.1 X-ray Photoelectron Spectroscopy

The surface compositions of glass powders both in as-received form and after heat treatment at 650°C for 2h, were analyzed with a SPECS ESCA X-ray photoelectron spectrometer with a monochromatized Al Kα source at 20 mA anode current with an electron-accelerating voltage of 10 kV with a pass energy of 80eV, a step size of 6eV and a dwell time of 150 ms. Quantitative surface compositions were determined from high resolution scans of the O(1s), C(1s), Si(2p), Na(KLL), Ca(2p), Na(1s), Ba(3d), Al(2p) and B(1s) spectral regions. Casa software was used to determine elemental sensitivity factors used for quantification. The charge corrections were performed based on C 1s line at 285.0 eV.

3.2.2 Surface Area Measurement (BET)

The surface area of all the glass powders was measured via a Surface Area Analyzer (Micromeritics Gemini). Specific surface areas of glass powders were determined using the multi-point BET method. The surface area in micropores and mesopores was measured using adsorption of chemically inert gases, such as nitrogen, argon or krypton. Nitrogen vapor adsorption data with relative vapor pressures (P/P_o) of 0.05, 0.10, 0.15, 0.20, 0.25 and 0.30 were obtained. Prior to surface area measurement, all glass powders were exposed to a high vacuum treatment at 200°C (outgassing) for 24h to remove all physisorbed species. The surface of glass powders were then conditioned with nitrogen (flowing stream) at 25°C for ~20 h. Following outgassing, the adsorption of nitrogen gas was measured in the relative equilibrium adsorption pressure (P/P_o) range of 0.05–0.30. In the expression (P/P_o), P is the absolute adsorption equilibrium pressure and P_o is the condensation pressure of nitrogen at laboratory conditions.

3.2.3 In-situ Infrared Analysis via Diffusion Reflectance Infrared Fourier Transformation Spectroscopy (DRIFTs)

In this study, DRIFTs was used for in situ analysis of glass powders in a temperature controlled Ar flowing cell. For this purpose, An IFS 66/s spectrometer (Bruker Optics, Billerica, MA) model FTIR system with a wide-band liquid nitrogen cooled mercury cadmium telluride (MCT) was coupled to a Praying Mantis type diffuse reflectance accessory along with a high temperature/vacuum (HTV) sample chamber (Thermo Spectra-Tech, Madison, WI). CaF_2 which has an IR cut-off below 1200 cm^{-1}, was used for the windows of the reaction cell (New Era Enterprises, Vineland, NJ). The IR reaction cell was purged with UHP Argon that was further purified using an oxygen/moisture/hydrocarbon filter (Restek, Bellefonte, PA), during measurement. The infrared spectra were acquired in the range of 4000-400 cm^{-1} at a resolution of 2cm^{-1} by 400 scans. For the diffusive reflectance measurements, glass powders without dilution with KBr were placed in a sample holder, then leveled by pressing with a flat spatula. All glass powders were ground and then sieved (< 10μm) prior to infrared analysis to reduce the particle

size effect of reflectance spectra. The obtained data are displayed as $-\log(R/R_0)$, where R is the reflectivity of the sample and R_0 is the reflectivity of a reference sample. The infrared spectrum of pure KBr, heat treated at 300°C for 30 min., followed by cooling to 150°C, was used as the reference spectrum.

The modified DRIFT spectrometer, described above, was used for desorption studies, in situ, during heating under Argon purging with a flow rate of 60 mL/min. After placing the glass powders in to sample holder in the HTV chamber, the infrared spectra of the glass powders were obtained at 25°C under Argon flow. Then, glass samples were exposed to in situ heating at 200, 450, 650°C for 30 min. and followed by cooling to 150°C. The infrared spectra of glass powders, subjected to heat treatment, were acquired after cooling to 150°C. The presence of physisorbed and chemisorbed water (released water from the glass powders) was monitored via the O-H stretching and H_2O bending regions of the infrared spectrum (3800-1600 cm^{-1}).

External Heat treatment of Glass Powders

Some of the glass powders were heated in an external furnace at temperatures higher than 600°C for a prolonged time (8 h). After heat treatment, DRIFTS analyses of the glass powders were conducted to determine the surface chemistry of glass.

3.2.4 Thermogravimetric Mass Spectroscopy (TG-MS)

In this study, mass spectroscopy coupled to TGA was used to obtain quantitative mass loss information about the evolved gases during desorption experiments. TG-MS spectroscopy provides ion intensity data for a specific m/e (mass/charge) component during a weight transition and converts it to a mass for that component. For quantitative analysis to be reliable with TG-MS spectroscopy, a calibration of the MS signal is essential. A component which exhibits stoichimoteric decomposition during heating and subsequently evolves only the gas species of interest was chosen for calibration of MS peak. In this study, it is interested in determination of evolved water vapor species and thus $CaC_2O_4.6H_2O$ (Calcium Oxalate), which evolves only water vapor during thermal decomposition, was used for calibration of MS signal [82]. It was observed that the intensity of MS signal was affected by operation parameters, such as flow rate of gas [82].

A TA Instrument Q50 TGA connected to a Pfeiffer Vacuum ThermoStar Mass Spectrometer by a pressure reducing system was used for TG-MS analysis of glass powders during in situ heating. The samples were heated in alumina crucibles at 10C°/min in a quartz-lined furnace to 650°C under helium flow. TGA analysis was carried out under atmospheric pressure while mass spectroscopy required low vacuum conditions. Therefore, the TGA was connected to the mass spectrometer by a two-stage pressure reducing system. Evolved gases from the TG furnace are fed to the MS through a heated steel capillary. The evolved gases flow in to vacuum chamber of

mass spectrometer through the orifice. The total pressure of the vacuum chamber was kept below 10^{-6} bar during the measurement. The transferred gas species were ionized by an axial beam electron source (100 eV). The ions were then separated according to their mass to charge ratio (m/z) via a quadrapole mass filter and then an Electron Multiplier (EM) detected the filtered ions. Figure 3.1 schematically describes the TG-MS (thermal analysis connected to mass spectrometer) system.

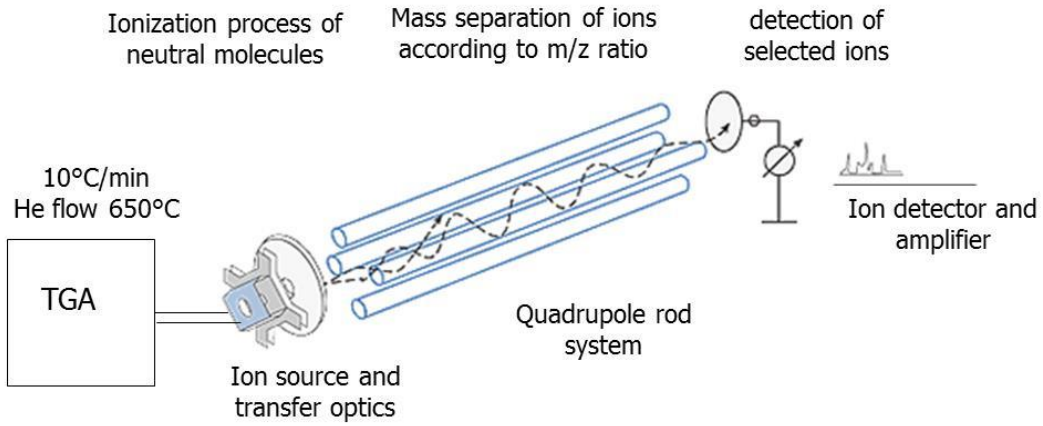

Figure 3.1 *TG-MS (thermal analysis connected to mass spectroscopy) system [82]*

Calibration Process

For calibration, $CaC_2O_4.6H_2O$ (Calcium Oxalate, Sigma-Aldrich), which exhibits well defined and characteristic thermal decomposition steps during heating, has been used to obtain calibration curves for quantitative analysis. It is well known that $CaC_2O_4.6H_2O$ thermally decomposes in three steps during heating in an inert atmosphere as shown below [82].

(1) $Ca+C_2O_4.6H_2O \longrightarrow CaC_2O_4+6H_2O$ (loss of water) ..Eq (3.1)

(2) $CaC_2O_4 \longrightarrow CaCO_3+CO$ (loss of carbon monoxide) …Eq (3.2)

(3) $CaCO_3 \longrightarrow CaO + CO_2$ (loss of carbon dioxide) … Eq (3.3)

In the first step, a stoichiometric compound CaC_2O_4 releases its physical water in the temperature range of 125-180°C, followed by transition to $CaCO_3$ (Calcium Carbonate) between 400 and 500°C through loss of CO (carbon monoxide). Finally in the third step, $CaCO_3$ is decomposed to CaO and CO_2 at around 650°C. The percentage of weight loss for water, carbon monoxide and carbon dioxide, corresponding to well resolved peaks and steps in MS and TGA data, respectively can be easily determined.

The TG-MS analysis of several distinct amounts of Calcium Oxalate, i.e. 0.5, 1.5, 5, 35 and 100 mg, was performed while heating to 650°C under helium gas flow with a heating rate of

10°C/min. The flow rate of inert helium gas in TG furnace is 90 mL/min. First, Calcium Oxalate powder was placed in an alumina crucible. The alumina crucible was cleaned through soaking 2% diluted Hydrochloric Acid (HCl, Sigma-Aldrich) and tared prior to analysis. The MS signals as well as weight losses corresponding to release of H_2O (m/z=18), CO (m/z=24) and CO_2 (m/z=48) were simultaneously monitored. The removal of water yielded a MS signal at m/z=18 and simultaneously, the percentage of weight loss in the range of 125-180°C. The percentage of weight loss for release of H_2O was converted to the weight of evolved H_2O by multiplying the initial amount of calcium oxalate with the percentage of weight loss. Then, the area under the MS signals for release of water as well as corresponding weight losses were determined. The calibration curve was obtained through plotting the area under MS for H_2O (m/z=18) as a function of corresponding weight loss for distinct amount of calcium oxalate powder. This calibration curve, shown in Figure 3.2 was used for determination of adsorbed water in/on glass powders.

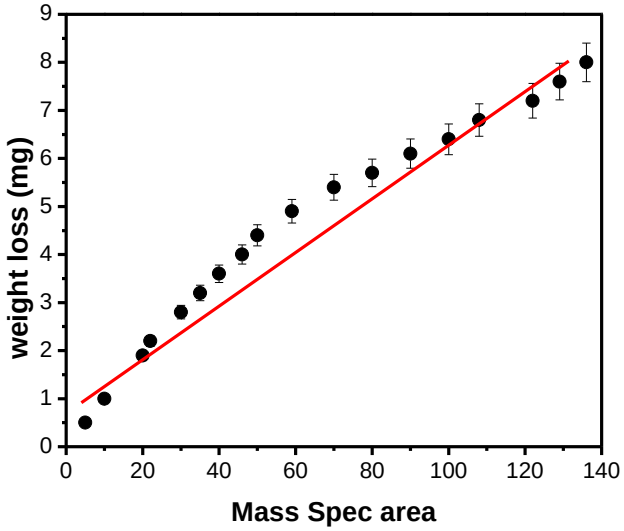

Figure 3.2 *$CaC_2O_4.6H_2O$ calibration curve obtained through plotting the area under MS for H_2O (m/z=18) as a function of corresponding weight loss for distinct amount of calcium oxalate powder. The line represents the linear fitted data.*

TG-MS Analysis of Powders

TG-MS analysis provides semi-quantitative information for released species during heating the glass samples. The amount of water adsorbed in/on glass samples was determined by this technique. Calibration and TG-MS measurements were performed under helium gas flow with a heating rate of 10°C/min. The flow rate of inert helium gas in TG furnace is 90 mL/min. The same operating parameters were used to minimize their effect on quantitative results.

TG-MS analyses of both dry- and wet-ground powders were performed in the TA Instrument Q50 TG furnace connected to a Pfeiffer Vacuum ThermoStar Mass Spectrometer. 344 mg of glass powder was placed in the alumina crucible and then the TG furnace was heated to 650°C

under helium flow with a heating rate of 10°C/min. The MS signal of evolved H_2O (m/z=18) and corresponding weight loss percentage were detected. The integrated area under the MS signal for H_2O was calculated via Origin 7.0 Program. Then the amount of water corresponding to integrated area under MS signal for H_2O was determined from the calibration curve.

3.3 D_2O Adsorption-Desorption Experiments on Glass Powders by in-situ DRIFT Spectroscopy

The physical adsorption of molecular water on glass surfaces preferentially occurs on hydroxyl groups (Si-OH, B-OH) groups. Thus, determination of surface hydroxyl concentration and reactivity is essential to understand surface properties as well as adsorption phenomena on glass. Additionally, most glasses have structural water, trapped as OH groups within the glass network. The infrared band corresponding to internal water overlaps with the infrared band of physically adsorbed water in the range of 3200-3500cm^{-1}. Therefore, distinguishing surface OH groups from both structurally bound water and physically adsorbed water is crucial for understanding surface chemistry, structure and properties. For this purpose, D_2O exchange experiments (named deuteration) were conducted on dry-ground glass powders, i.e. fused silica, fused quartz, soda-lime-silica, Ba-boroaluminosilicate and Ba-silicate using in-situ DRIFT Spectroscopy. Deuteration is basically the isotopic exchange reaction of hydrogen atoms of surface hydroxyl groups for deuterium in physisorbed D_2O [65]. This isotopic exchange process is highly favored because the mass of the D atom is much higher than that of the H atom. The deuteration reaction is described below.

$$\equiv Si\text{-}OH + D_2O \longrightarrow \equiv Si\text{-}OD + HDO \qquad \text{Eq (3.4)}$$

D_2O adsorption experiments were conducted on dry-ground glass powders of fused silica, fused quartz, soda-lime-silica, Ba-boroaluminosilicate and Ba-silicate. An IFS 66/s spectrometer (Bruker Optics, Billerica, MA) model FTIR system with a wide-band liquid nitrogen cooled mercury cadmium telluride (MCT) connected to a diffuse reflectance accessory along with a high temperature/vacuum (HTV) sample chamber (Thermo Spectra-Tech, Madison, WI) was used to monitor simultaneous changes in the surface of glass while adsorbing D_2O vapor. For in situ D_2O vapor dosing experiments, the HTV attached DRIFTs was further modified with a GC splitless injector system (Restek). The GC splitless injector system consisted of stainless steel, 1/4″ stainless steel nuts, 1/4″ graphite ferrules and a welded shell. The heater tape, connected to temperature controller and kept at 150°C, was wrapped around the GC injector port for vaporization of liquid D_2O. For insulation of the GC injector port, glass wool was used. A schematic representation of the in-situ DRIFTs system is given in Figure 3.3.

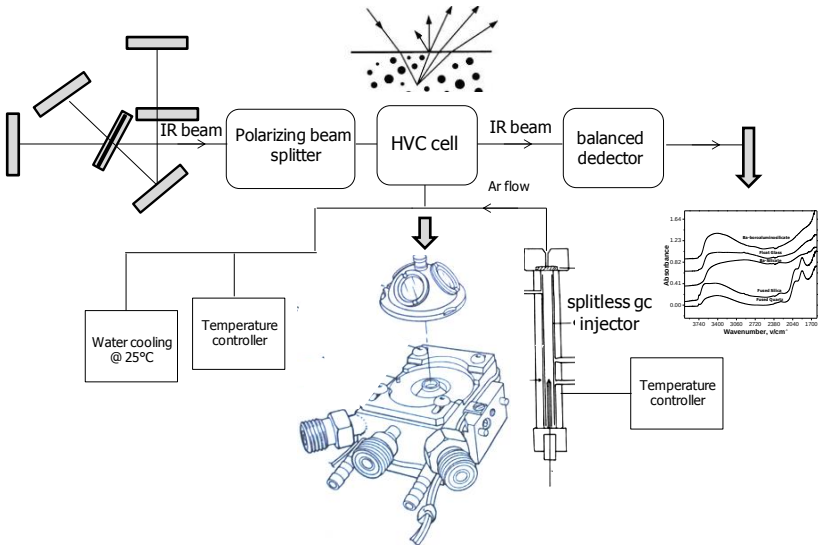

Figure 3.3 *A schematic representation of modified DRIFTS system for in-situ adsorption experiments*

Prior to injection of a controlled dose of D_2O vapor, the glass powders were exposed to in situ heating at 150, 450, 600 and 800°C for 30 min. under Argon flow in the HTV reaction chamber to remove physically adsorbed water and to condense silanols. Pretreatment temperatures for different type of glasses were chosen with respect to their glass transition temperature (T_g). After in-situ heat treatment of glass powder samples, they were cooled to room temperature. Then, D_2O (Deuterium Oxide, Sigma-Aldrich) was vaporized and fed into the reaction chamber under Argon purging at 25°C. Argon, at a flow rate of 60 mL/min, was used as a carrier gas by diverting the D_2O vapor through the reaction cell. The DRIFT spectra of the glass powders were collected simultaneously in the range of 4000-400 cm^{-1} at a resolution of 2 cm^{-1} by 400 scans. The changes in the spectra were monitored simultaneously. After controlled amounts of D_2O, i.e 1, 2, 5, 10, 15, 25, 50, 75, 100, 200, 300, 500, 750, 1000, 1250, 1500 and 1750 µl were injected sequentially into the reaction chamber, the saturation of the surface was determined for each glass composition by observing the abrupt change in the spectra or resulting D_2O vapor condensation on the CaF_2 windows in the chamber. The saturation point for adsorption of the D_2O vapor showed a dependence on the glass composition and the pretreatment temperature. Similar D_2O vapor adsorption experiments were conducted on pure KBr powder as a reference.

3.4 Water Adsorption Experiments on Glass Powders

TG-MS Spectroscopy

Readsorption of atmospheric moisture on heat treated glass powder samples was investigated by TG-MS spectroscopy. The amount of moisture readsorbed on pretreated glass powder was determined after exposing them to ambient air for 1 day, 1 week and 1 month. In the first step, glass powder placed in the alumina crucible was heated to 650°C in the TG furnace under helium flow with a heating rate of 10°C/min and the evolved MS signal as well as the corresponding weight loss for water release was monitored. Then, the glass samples was kept inside the TG furnace to prevent it from exposure to atmospheric water and the TG-MS analysis with same

operation parameters was conducted again on glass powder to ensure that no water left on/in glass powders after heat treatment at 650°C. Then, glass powders were exposed to atmospheric moisture for 1 day, 1week and 1 month. TG-MS analysis of the glass powders were performed again to determine the amount of water readsorbed on glass powders during their stay in ambient air.

DRIFT Spectroscopy

Water adsorption experiments were conducted on dry-ground glass powders of fused silica, fused quartz, soda-lime-silica, Ba-boroaluminosilicate and Ba-silicate by in-situ DRIFT Spectrometer modified with GC injector. Prior to dosing of DI (deionized) water, the glass powders were exposed to in-situ heating at 150, 450 and 600°C for 30 min. under Argon flow in the reaction chamber to remove the adsorbed water. Pretreatment temperatures for different type of glasses were chosen with respect to their glass transition temperature (T_g). After in-situ heat treatment of glass samples, they were cooled to room temperature. Then, D_2O (Deuterium Oxide, Sigma-Aldrich) was vaporized and fed into the reaction chamber under Argon purging at 25°C. Argon flow rate was 60 mL/min and it was used as a carrier gas for transference of water vapor through the reaction cell. The DRIFT spectra of glass powders were collected simultaneously in the range of 4000-400 cm^{-1} at a resolution of 2 cm^{-1} by 400 scans. The change in surface of glass powders was monitored simultaneously with DRIFT spectrometer during injection of water vapor in to HVT reaction chamber. 1, 2, 5, 10, 15, 25, 50, 75, 100, 200, 300, 400µl of DI water was injected sequentially into the reaction chamber. Similar water adsorption experiments were conducted on pure KBr powder as a reference.

Chapter 4

DRY-GROUND SILICA and SILICATE GLASS POWDERS

4.1 Introduction

The water adsorption properties on silica and silicate glasses are quite different due to structural variation of adsorption sites on their surfaces. In general, strained bonds and coordination defects on the silica surface can react with water to form silanol groups, and further interaction of silica surface with water is limited by the number of these silanol groups. The surface of multicomponent glasses, on the other hand, involves additional adsorption sites, such as modifier ions, and non-bridging oxygen groups, which can contribute to silanol formation.

Moreover, the formation of silanol groups in the case of silica is limited to a few atomic layers of surface because the bulk silica structure is very resistant to attack by water. On the other hand, the bulk glass composition on multicomponent glasses has a more profound effect on adsorption of water. The extent of water adsorption depth is not limited to the outermost layer and is directly related to the amount of alkali in glass [4]. The contribution of in-depth bulk structure to adsorption of water on multicomponent glass makes understanding water-glass interactions more complicated. When alkali or alkaline iozns are present in silicate glasses, each alkali and alkaline earth ion can generate one and two non-bridging oxygen, respectively to compensate their charge in the silicate network. These non-bridging oxygen ions act as active surface sites and can react to water moisture to form silanol groups, giving off modifier (M^{+}, M^{++}) and OH^{-} ions [36]. This reaction first starts at the surface of glass where a high number of non-bridging are present. Then, it can continue in the diffusion channels to form alkali depleted porous layer, which is less durable against attack by water.

The extent of hydration in bulk of the multicomponent glasses strongly dependent on the concentration and type of modifier ions, the bond strength between the modifier and non-bridging oxygen ions, and the presence of network intermediates (B_2O_3 and Al_2O_3). For example, Ba^{2+} ions can generate non-bridging oxygen ions, leading to formation of more diffusion channels and thus enhancing the hydration depth. Bulk diffusion is also involved when the amount of modifier ions is high enough that an open silicate network allows free ions to move the surface to react with water.

Besides the network modifiers and intermediates, the bulk water, mostly in the form of H_2O molecules or OH groups within and attached to the glass network, are also a factor. These

internal water molecules act as modifier ions in the silicate network. They can break the Si-O-Si bonds and form non-bridging oxygen in the glass network. The formation of new non-bridging oxygens in the glass structure promotes physisorption and bulk hydration.

In this study, it is mainly interested in surface hydration behavior in a variety of multicomponent glasses. However, most of the techniques, including (DRIFTs and TG-MS) provide information on both internal and surface water-related species. There are some commonly used techniques, such as Karl Fisher titration and D_2O exchange experiments in the literature to distinguish internal and surface water species in/on glass. In this study, we used D_2O exchange experiments by modified in-situ DRIFT spectroscopy to differentiate surface water from structural water as well as to understand how the bulk chemical composition affects the type and fraction of possible sites for adsorption of water on glass surface. For this purpose, dry ground Ba-silicate, Ba-boroaluminosilicate, float glass, fused silica and fused quartz were used. After D_2O exchange experiments, the water-related species were identified by in-situ desorption experiments in DRIFTs. Water adsorption phenomena on different silica and multicomponent glasses are described based on structural variation in glass network with the type and concentration of modifier ions as well as the presence of as B_2O_3, Al_2O_3 and internal water. Moreover, the concentration of water-related species on/in silica and silicate glasses was determined by TG-MS.

4.2 Results

4.2.1 BET *(Brauner-Emmett-Teller)* Surface Area Analysis

Table 4.1 shows the surface area of all glass powders before and after heat treatment at 650°C for 2h. The surface area of as-prepared glass powders are 3.42, 2.37, 3.41, 9.35, and 6.66 m^2/g for

Table 4.1 *BET surface area of Ba-boroaluminosilicate, Ba-silicate, fused silica, fused quartz powders before and after heat treatment at 650°C for 2h*

Surface Area (m^2/g)	**25°C**	**650°C**
Ba-boroaluminosilicate	3.42±0.06	2.37 ±0.03
Float Glass	2.37±0.06	1.65±0.05
Ba-silicate	3.41±0.04	2.94±0.02
Fused Silica	9.35±0.03	8.94±0.05
Fused Quartz	6.66±0.07	6.09±0.04

Ba-boroaluminosilicate glass, float glass, Ba-silicate glass, fused silica and fused quartz, respectively.

The variation in the surface area of glass powders is due to hand grinding with mortar and pestle. Although all glass powders were ground for the same amount of time, the resultant particle size depends on the applied pressure of the mortar. Heat treatment at 650°C resulted in a decrease in surface area of glass powders. The surface area of heat treated glass powders at 650°C are 2.37, 1.65, 2.94, 8.94, and 6.09 m^2/g for Ba-boroaluminosilicate glass, float glass, Ba-silicate glass, fused silica and fused quartz, respectively.

4.2.2 X-ray Photoelectron Spectroscopy (XPS) Analysis

XPS analyses of the glass powders showed the presence of elements such as C, Si, O and Al, B, Ba, Na, Ca, Mg in some cases. Table 4.2 summarizes the chemical composition of glass powders having different chemical compositions, determined from quantitative analysis of high resolution regional scans. There is no significant change in chemical composition of the glass powders after thermal treatment at 650°C. The atomic concentration of modifier ions like Ba, Na in Ba-boroaluminosilicate and float glass remains nearly constant after heat treatment.

High resolution XPS analyses after heat treatment at 200, 450 and 650°C were performed to determine the chemical composition of the glass powders. Figure 4.1 exhibits the high resolution O(1s) and modifier ions like Na(1s) and Ba(3d) present in glass powders. Figure 4.1a depicts the high resolution Ba(3d) and Na(1s) regions of Ba-boroaluminosilicate and float glass respectively, in as-prepared condition as well as after heat treatment at 650°C. The binding energy of Ba(3d) for as–prepared Ba-silicate and Ba-boroaluminosilicate glasses was found 779.7 and 780.5 eV, respectively. The position of Ba(3d) peak shifted to 779.4 and 780.9 eV for Ba-silicate and Ba-boroaluminosilicate glasses, respectively after heat treatment at 650°C. Moreover, the binding energy of Na(1s) peak for as-prepared float glass is 1071.8 eV and remains constant after heat treatment at 650°C.

Figure 4.1b shows the high resolution O(1s) region for Ba-boroaluminosilicate, float glass, fused silica and fused quartz. As shown in Figure 4.1b, the position and the full width at half-max (FWHM) of O(1s) significantly changes with the chemical composition of glass powders. For fused silica and quartz, the position of O(1s) was found 532.8 eV. The position of O(1s) shifted to lower binding energy (531.8eV) for Ba-boroaluminosilicate glass. For float glass, on the other hand, a shoulder peak located at 530.4 eV emerged in addition to an intense O(1s) peak at 532.2 eV. The full width at half-max (FWHM) of modifier-containing glass powders like Ba-boroaluminosilicate and float glasses are greater than that for the fused silica and fused quartz. The binding energy change and related peak position shifts in the XPS spectra suggest that the chemical state of oxygen changes with chemical composition.

Table 4.2 *Approximate chemical composition of the Ba-boroaluminosilicate, Ba-silicate, fused silica, and fused quartz powders before and after heat treatment at 650°C for 2h*

25°C	O (at.%)		Ca (at.%)		Mg (at.%)		B (at.%)		Si (at.%)		Al (at.%)		Ba (at.%)		Na (at.%)	
	surface	*Bulk*	*surface*	*bulk*	*surface*	*bulk*	*surface*	*Bulk*	*surface*	*bulk*	*surface*	*bulk*	*surface*	*bulk*	*surface*	*bulk*
Ba-boroaluminosilicate	57	63					12.7	9	23.2	18.9	5.9	5.4	1.2	3.6		
Float Glass	61	60	2.1	3.3	2.4	1.6			29.9	25.2					4.8	9.6
Ba-silicate	67.6	62.6							23.3	25			9.1	12.5		
Fused Silica	62	60							38	40						
Fused Quartz	40								60							

650°C (surface)	O (at.%)	Ca (at.%)	Mg (at.%)	B (at.%)	Si (at.%)	Al (at.%)	Ba (at.%)	Na (at.%)
Ba-boroaluminosilicate	57.9			12.7	22.6	5.71	1.09	
Float Glass	61.6	2.03	2.67		29.4			4.3
Ba-silicate	73.3				18.1			
Fused Silica	60.9				39.1			
Fused Quartz	60.7				39.3			

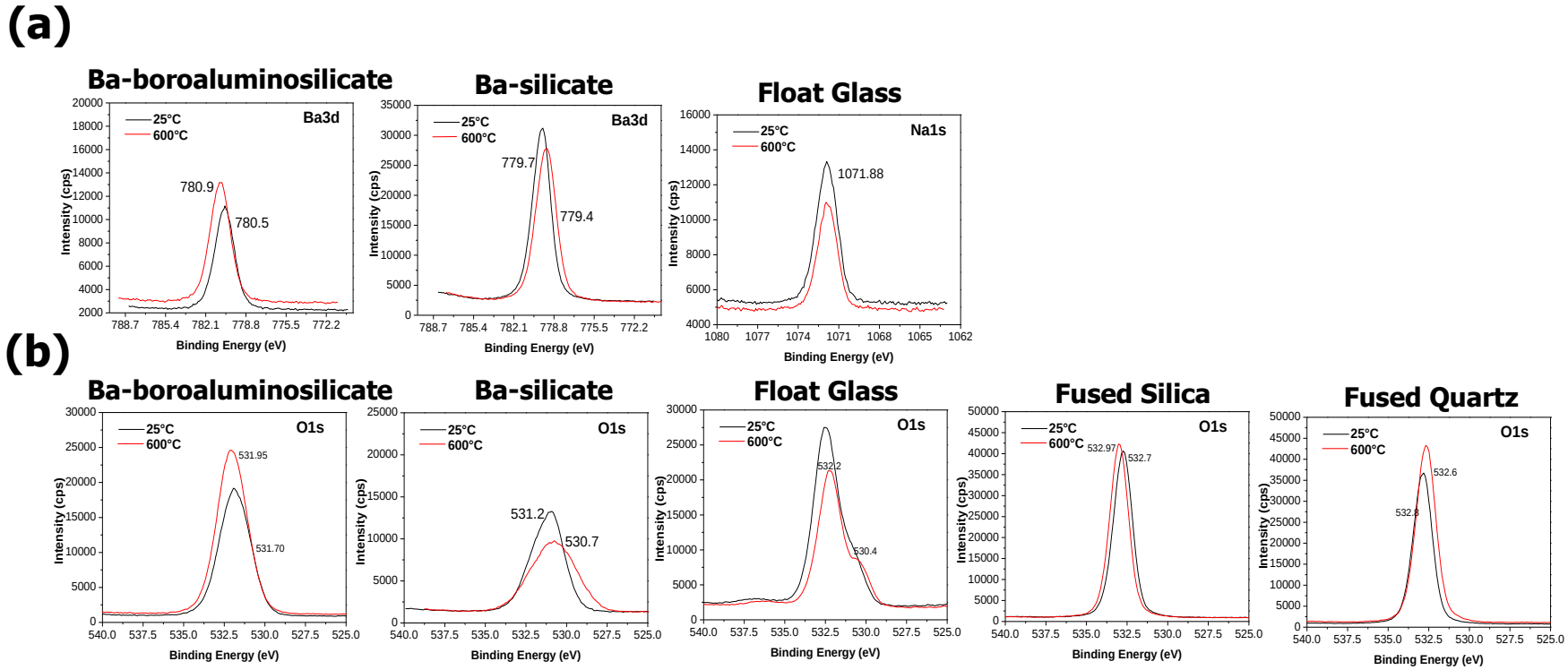

Figure 4.1 *High resolution (a) Ba 3d, Na 1s spectra of Ba-boroaluminosilicate, Ba-silicate, and float glass, respectively (b) O 1s spectra of Ba-boroaluminosilicate, Ba-silicate, float glass, fused silica, and fused quartz in as-prepared conditions as well as after heat treatment at 650°C*

4.2.3 Thermogravimetric Mass Spectroscopy (TG-MS)

Figure 4.2 shows the TG-MS spectra of glasses with different chemical compositions. The spectra were obtained by collecting the change in sample weight and ionized product gases (by Mass spectroscopy) simultaneously upon heating to 650°C. Figure 4.2a exhibits the change in sample weight during heating to 650°C with a heating rate of 10°C/min. As shown in Figure 4.2a, the decrease in sample weight of float and Ba-silicate glasses during heating is much more than Ba-boroaluminosilicate, fused silica and fused quartz counterparts. The mass change was detected as 1.26%, 1.08%, 0.48%, 0.45% and 0.38% for Ba-silicate, float glass, Ba-boroaluminosilicate glass, fused silica and fused quartz, respectively. Figure 4.2b shows mass signals for evolved H_2O (m/z=18) vapor for glasses with different chemical compositions, collected simultaneously upon heating to 650°C. Two different mass signals attributed to H_2O (m/z=18) were found for multicomponent silicate powders. First the H_2O signal that emerged around 120-140°C was assigned to physically adsorbed water; the second water signal appeared at around 400°C, corresponding to internal water and vicinal Si-OH groups. The intensity of H_2O signals at 130°C, attributed to physically adsorbed water, was found highest for Ba-silicate and it is decreasing in the order of float glass, Ba-boroaluminosilicate glass. The second H_2O signal at around 400°C, attributed to internal water and vicinal Si-OH groups, is more obvious in Float Glass compared to Ba-silicate and Ba-boroaluminosilicate glass powders. For fused silica and quartz, on the other hand, the H_2O (m/z=18) signal attributed to physically adsorbed water appeared at lower temperature around 100°C with lower intensity. The second H_2O signal, corresponding to internal water was only observed for fused silica between 200-600°C.

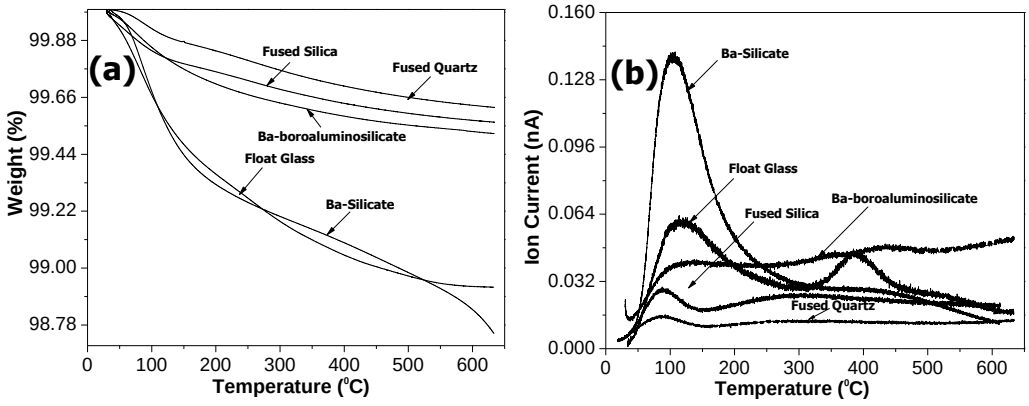

Figure 4.2 (a) *TG plots and corresponding mass signals for evolved H2O (m/z=18) for glass powders with different chemical compositions. The data were collected upon simultaneous heating to 650°C*

Water Adsorption on Dehydroxylated Glass Powders upon Exposure to Atmospheric Moisture

Rehydration of dehydroxylated glass powders was quantitatively evaluated by TG-MS spectroscopy as a function of time, i.e. 1 day, 1week and 1 month. Figure 4.3 exhibits the results of TG-MS spectra of dehydroxylated glasses after exposing to open atmosphere for distinct times. The first and second runs represent the TG-MS spectra of glass powders, collected upon sequential heat treatments to 650°C in the TG furnace. The purpose of second heat treatment was to ensure there is minimal or no water left on/in the dehydroxylated glass powders. After dehydroxylation process, glass powders were exposed to ambient air for distinct times. 1 day, 1 week and 1 month in Figure 4.3 represent the exposure time of dehydroxylated glass powders to ambient air. As shown in Figure 4.3a, there is a gradual increase in percentage of water loss as the exposure time of glass powders to ambient air becomes longer. The percentage of water in/on partially hydroxylated glass powders, recovered upon exposure to ambient air was found higher for fused silica and Ba-silicate. Additionally all glass powders exhibit gradual increase in the percentage of weight loss corresponding to H_2O with longer exposure times. Figure 4.3b illustrates the MS signals for evolved H_2O gas during TG-MS analysis after exposure to ambient air for distinct times. As shown in Figure 4.3b, the MS signals, attributed to both physically adsorbed water and internal water, disappeared after the second heat treatment at 650°C for all glass powders. After exposure to ambient air, the only MS signal corresponded to physically adsorbed water started to reappear for all glass powders (except for fused silica) and the intensity of the MS signal for release of physically adsorbed water increased with exposure time. On the other hand, for fused silica, the additional MS signal, attributed to internal water reappeared and it became more enhanced with increase in exposure time. After 1 month exposure to ambient atmosphere, the intensity of H_2O signals, for fused silica and Ba-silicate glass, reached its original value, achieved upon first heat treatment to 650°C. On the other hand, the MS spectra, collected during the first heat treatment at 650°C and after 1 month exposure to atmospheric moisture shows apparent difference for Ba-boroaluminosilicate, float glass and fused quartz powders.

Quantitative analysis to determine the number of H_2O molecules released upon heating of glass powders to 650°C was conducted after exposure to ambient air for distinct times. For quantitative analysis, a $CaC_2O_4.6H_2O$ calibration curve was used to estimate the corresponding value of water loss, evolved upon heating of glass powders to 650°C. The area under MS signal was calculated and corresponding water amount for calculated integrated area was determined from $CaC_2O_4.6H_2O$ calibration curve. The mass loss for evolved H_2O then converted to the number of H_2O molecules per nm^2. Table 4.3 shows the number of H_2O molecules per nm^2 during first and second heat treatment at 650°C as well as after exposure to ambient air for 1 day, 1 week and 1 month.

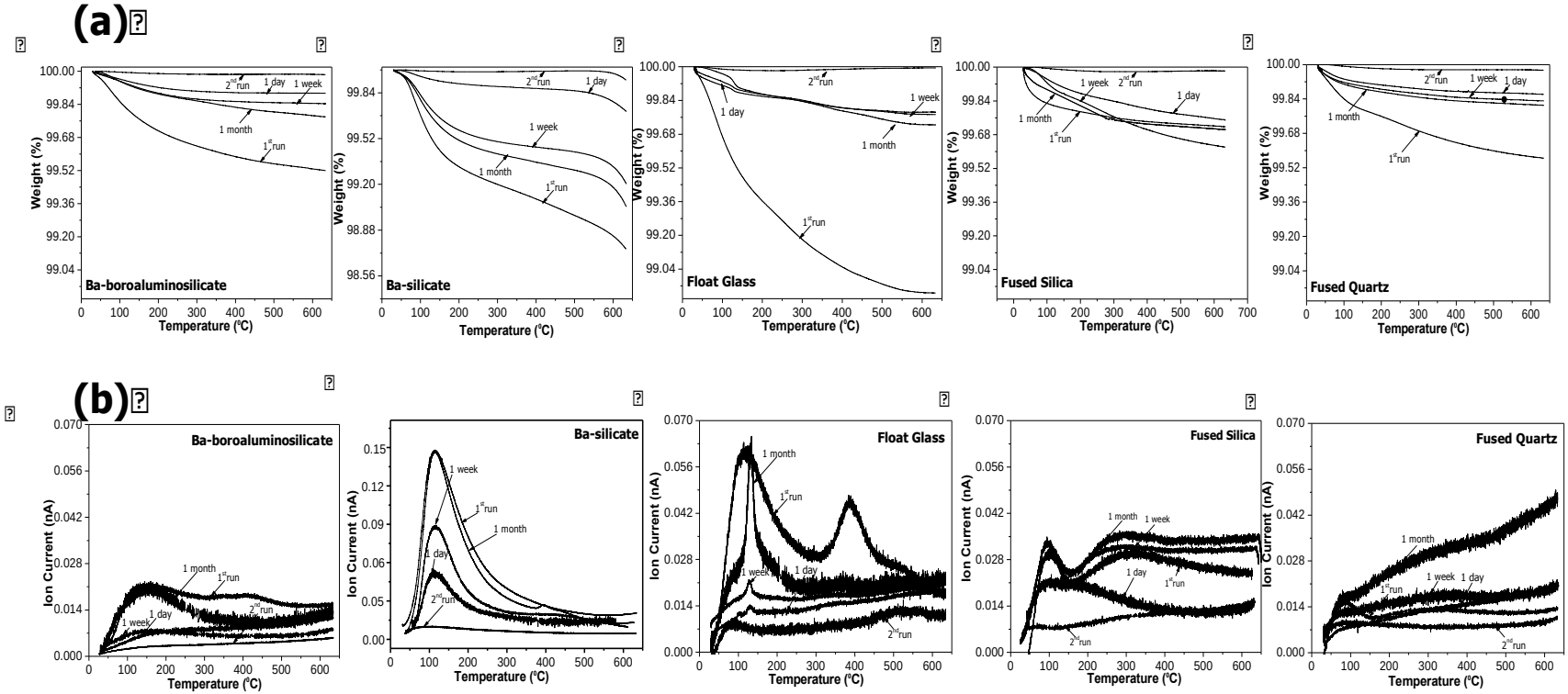

Figure 4.3 *(a) TG plots and (b) corresponding mass signals for evolved H_2O (m/z=18) for glass powders with different chemical compositions upon sequential heat treatments to 650°C (1st and 2nd run) as well as after exposure to atmospheric moisture for distinct times, i.e. 1 day, 1 week, and 1 month.*

Table 4.3 *The amount of water released upon heat treatment of glass powders with distinct chemical compositions during first and second heat treatments at 650°C as well as after exposure to atmospheric moisture for 1 day, 1 week, and 1 month (unit: the number of H_2O molecules per nm^2)*

Mass/Surface Area	1st run	2nd run	1 day	1 week	1 month	Surface area
Ba-boroaluminosilicate	6.5	0.01	1.9	3.0	4.2	3.42 m²/g
Float Glass	10.4	0.01	2.6	4.1	5.9	2.37 m²/g
Ba-silicate	11.8	0.01	5.4	8.7	10.9	3.41 m²/g
Fused Silica	3.9	0.01	1.8	2.4	3.6	9.35 m²/g
Fused Quartz	3.2	0.01	1.3	1.9	3.1	6.66 m²/g

The number of H_2O molecules per nm^2 was found 6.5, 10.4, 11.8, 3.9 and 3.2 for Ba-boroaluminosilicate, float glass, Ba-silicate, fused silica and fused quartz upon heat treatment at 650°C. The number of H_2O molecules per nm^2 is very close to 0 after the second heat treatment at 650°C. Exposure of glass powders to atmospheric moisture resulted in an increase in the amount of water in/on glass powders. After 1 day of exposure to ambient air the number of H_2O molecules per nm^2 was detected as 1.9, 2.6, 5.4, 1.8 and 1.3 for Ba-boroaluminosilicate, float glass, Ba-silicate, fused silica and fused quartz, respectively. The number of H_2O molecules per nm^2 increased to 3, 4.1, 8.7, 2.4 and 1.9 after 1 week exposure to atmospheric moisture and finally, it reached to 4.2, 5.9, 10.9, 3.6 and 0.05 for Ba-boroaluminosilicate, float glass, Ba-silicate, fused silica and fused quartz, respectively after 1 month exposure to ambient air.

4.2.3 Diffuse Reflectance Infrared Spectroscopy (DRIFTs)

Dehydration and Dehydroxylation Studies

High temperature DRIFTs analysis of glass samples during in situ heating to 600°C with a heating rate of 10°C/min was conducted simultaneously under Argon flow to detect water-related IR bands. The DRIFT spectra of glass samples were collected at 150°C after heating at 200, 400 and 600°C for 30 min. Figure 4.4 illustrates the DRIFT spectra of glass powders at 25°C as well as after in situ heating at 200, 400 and 600°C for 30 min. Figure 4.4a shows the DRIFT spectra of glass powders with different chemical compositions at 25°C. All glass powders except for Ba-silicate, exhibit a small sharp band at ≈3737 cm^{-1}. This absorption band is attributed to the primary OH stretching vibration of isolated free Si-OH groups [35]. Silica and multicomponent glasses exhibit some differences in their IR spectra. Fused silica and fused quartz exhibit relatively broad band between 3715-2800 cm^{-1}, with two distinct maxima centered at 3600 and 3400 cm^{-1}, attributed to structural water inside silica network and physically adsorbed water on glass surface, respectively, was observed [56]. On the other hand, float and Ba-silicate glass powders present very broad absorption peak in the range of 3720 and 2400 cm^{-1}, while Ba-boroaluminosilicate glass exhibits relatively narrower band located between 3720 and 2800 cm^{-1}.

In addition Ba-silicate glass powder presents two additional IR bands located at 1750 and 2452 cm^{-1}, corresponding to formation of $BaCO_3$ compound.

Figure 4.4b depicts the DRIFT spectra of glass powders having distinct chemical compositions, after in situ heat treatment at 200°C for 30 min. As shown in the Figure 4.4b, for all glass powders, heat treatment at 200°C leads to the appearance of more well-defined IR band at 3737 cm^{-1}, assigned to free isolated Si-OH groups, accompanied by a significant decrease in intensity of broad IR peak region between 2400 and 3600cm^{-1}. Meanwhile, the lower wavelength region (3200-3400cm^{-1}) of a broad band (2800-3700 cm^{-1}) for fused silica and quartz disappeared after heat treatment at 200°C while there is no considerable change in the width of broad band for modifier containing glass powders. The intensity of the band at 1750 and 2452 cm^{-1} suggests $BaCO_3$ formation, increases after heating to 200°C.

Figure 4.4c illustrates the DRIFT spectra of glass powders with different chemical composition after heating to 400°C. Heat treatment at 400°C resulted in a further increase in intensity of free isolated Si-OH band, and a gradual decrease in intensity of broad band located between 2400 and 3600cm^{-1} in DRIFT spectra of all glass powders. The decrease in intensity of the broad band between 2400 and 3600 cm^{-1} is much more severe in float glass and Ba-silicate glass powders compared to other glass powders. The width of the broad band between 3700 and 2800 cm^{-1} for fused silica and quartz continued to decrease after heat treatment at 400°C.

Figure 4.4d exhibits the DRIFT spectra of glass powders, having different chemical compositions, after heat treatment at 600°C. The intensity of an IR band at 3737 cm^{-1}, assigned to free isolated Si-OH increased further after heat treatment at 600°C. There is a considerable difference in the intensity of the broad band in the 2400-3600cm^{-1} spectral region, as a function of the chemical composition of glass. For fused silica and quartz, the intensity of this broad band, corresponding to structural and physically adsorbed water is much higher compared to modifier containing glasses. Heating to 600°C reveals an additional $BaCO_3$ band at 2822 cm^{-1} in addition to 1750 and 2452 cm^{-1} in Ba-silicate glass.

Deuteration Studies

Dehydration studies of glass powders provide information on both structural and surface water-related species. The broad band located between 2400-3600 cm^{-1} may involve different type of water related species, i.e. physically adsorbed water, structural water trapped as OH and OH groups H-bonded to NBO (non-bridging oxygen) and Si (Si-OH). Because the main interest is to understand water adsorption phenomena on the glass surfaces, D_2O exchange studies were performed to differentiate surface water from structural water as well as to understand how the chemical composition affects the type and fraction of possible sites for adsorption of water on glass surfaces

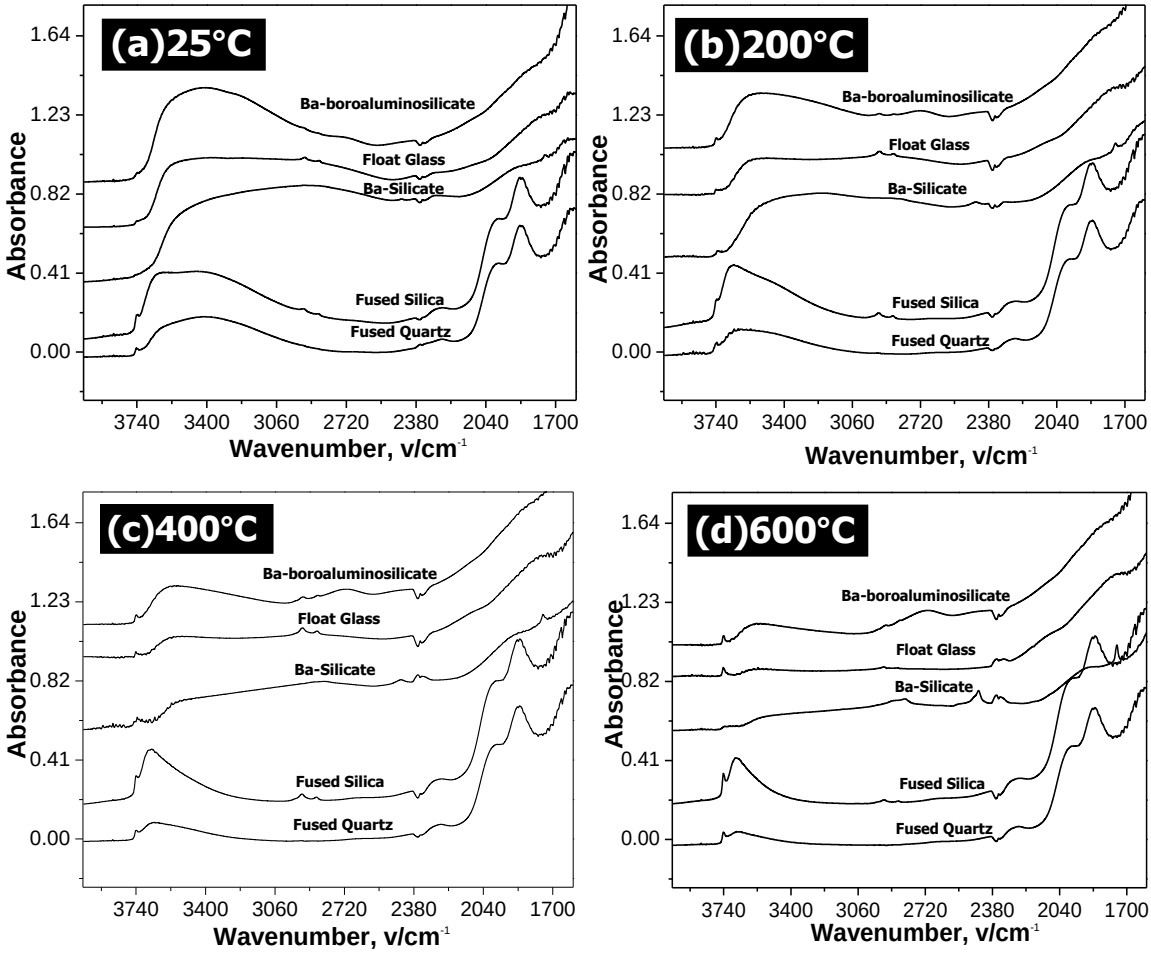

Figure 4.4 *DRIFT spectra of Ba-boroaluminosilicate, float glass, Ba-silicate, fused silica, and fused quartz powders (a) in as-prepared conditions and after heating at (b) 200, (c) 400, and (d) 600°C for 30 min.*

Figure 4.5 shows the IR spectra of Ba-silicate, Ba-boroaluminosilicate, float glass, fused silica and fused quartz powders, after reaction of D_2O in situ DRIFT cell under Argon flow. The IR spectra in the range of 4000-1500 cm^{-1} were collected at room temperature after reaction of pretreated glass powders at 150, 450 and 600°C with D_2O. The highest pretreatment temperature for different glass compositions was chosen depending on their glass transition temperature (T_g). Figure 4.5a shows the IR spectra of multicomponent glasses, i.e. Ba-silicate, float and Ba-boroaluminosilicate glasses after reaction of D_2O in situ DRIFT cell. The IR spectra of KBr after reaction of pure D_2O at 25°C is also given as a reference spectrum in Figure 4.5a. As shown in Figure 4.5a, the reactivity of D_2O with water related species on glass surface is significantly affected by chemical composition of glass. For all glass powders pretreated at distinct temperatures, the free isolated Si-OH IR band at 3737cm^{-1} vanishes after reaction of D_2O, accompanied by appearance of new IR band in 2400-2780 cm^{-1} spectral regions with maxima at 2758 cm^{-1} attributed to Si-OD stretching vibration [65]. The formation of new Si-OD band indicates the extent of D_2O exchange reaction with water species on the surface of glass powders. The disappearance of isolated Si-OH band indicates that all free Si-OH groups on glass

surface can undergo exchange reaction with D_2O. In contrast to free Si-OH groups, structural water remains after exchange reaction with D_2O, as evidenced by the presence of a broad band in 3650-3450 cm^{-1} spectral regions.

The extent of D_2O exchange reaction with water species in the range of 3650-3400cm^{-1} is strongly dependent on chemical composition as well as pretreatment temperature (Figure 4.5a.). Ba-boroaluminosilicate glass powder pretreated at 150°C exhibits noticeable decrease in the intensity of IR band in the 3650-3400 cm^{-1} region, accompanied by the appearance of high intensity Si-OD band at 2758 cm^{-1}. However, pretreatment of Ba-boroaluminosilicate glass at 650°C resulted in a slight increase in the intensity of the IR band between 3650 and 3400 cm^{-1} region after exchange reaction with D_2O. For float glass, after pretreatment at both 150 and 450°C, the relatively small decrease was observed in IR band between 3650-3400 cm^{-1} after the D_2O exchange reaction. For the Ba-Silicate glasses on the other hand, the increase in pretreatment temperature leads to enhancement in the D_2O exchange reaction.

Figure 4.5b depicts the IR spectra of fused silica and quartz after reaction in the D_2O in situ DRIFT cell. The IR spectra of KBr after reaction of pure D_2O at 25°C is also given as a reference in Figure 4.5b. Similar to multicomponent glass powders, deuteration of fused silica and quartz leads to disappearance of the isolated Si-OH band located at 3737 cm^{-1}, accompanied by emergence of a new IR band centered at 2758 cm^{-1}, corresponding to the Si-OD stretching vibration. The extent of deuteration is higher compared to multicomponent glasses and becomes lower with increase in pretreatment temperature.

Based on the assumption that IR bands in the H_2O region of the spectra after reaction of D_2O represent structural water in silicate network, the IR spectra of glass powders, involving both structural and surface related water species (Figure 4.4) were subtracted from the IR spectra of pretreated glass powders after interaction with D_2O (Figure 4.5) to obtain IR spectra for glass powders, consisting of only surface-related water species (Figure 4.6). For this purpose, IR spectra of glass powders in the as-prepared condition as well as after in-situ heat treatment were subtracted from IR spectra of pretreated glass powders after D_2O reaction. Figure 4.6a illustrates the IR spectra of glass powders with different chemical compositions at 25°C. Isolated Si-OHgroups were only observed for fused silica and quartz at 25°C. Additionally, a broad IR band centered at 3400 cm^{-1}, assigned to physically adsorbed water was seen in IR spectra of fused silica and quartz. The multicomponent glass powders on the other hand exhibit only a broad band between 3650-2750 cm^{-1}. For Ba-silicate and float glass powders, this broad band presents two maxima located at 3600 and 2850 cm^{-1}, attributed to H bonded OH groups and NBO (non-bridging oxygen), respectively. As shown in Figure 4.6b, heat treatment at 200°C leads to appearance of isolated Si-OH band in multicomponent glass and decrease in a broad IR band, corresponding to physically adsorbed water and H bonded OH species. The decrease in this broad band is more obvious in the multicomponent glass powders compared to fused silica and

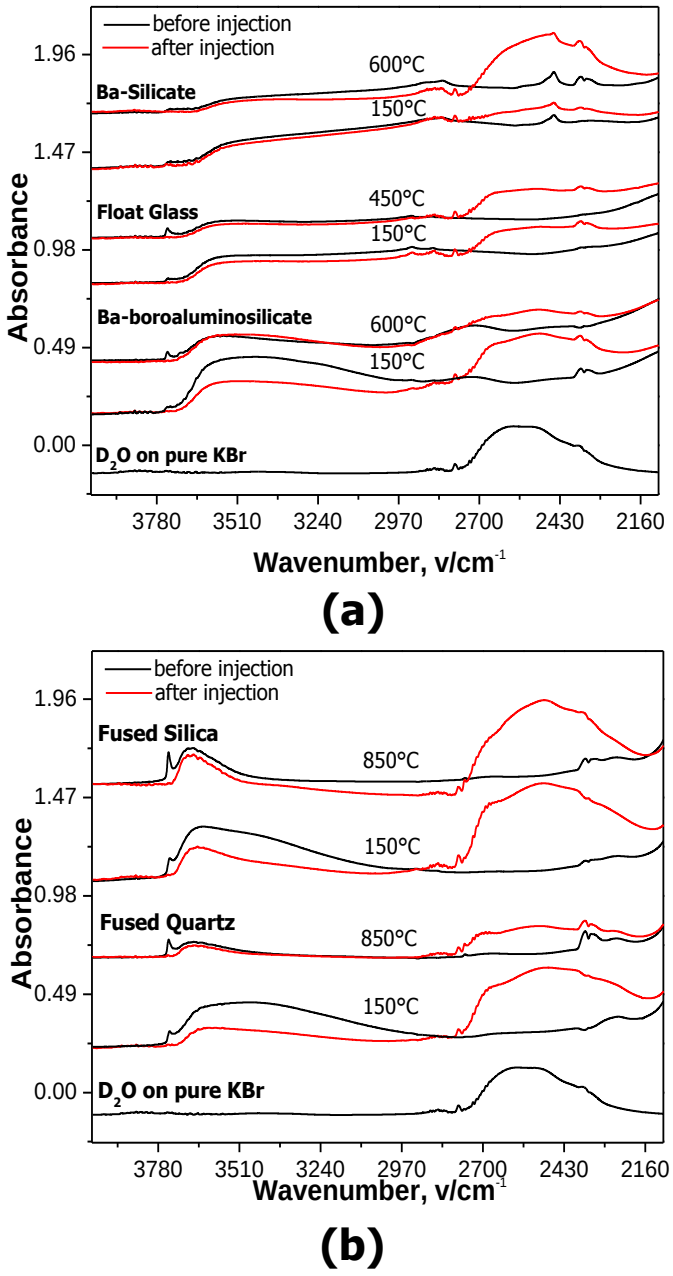

Figure 4.5 *DRIFT spectra of (a) heat treated Ba-boroaluminosilicate, float glass, and Ba-silicate powders and (b) fused silica and fused quartz , before and after reaction of D_2O in situ DRIFT cell*

quartz. Further heating to 400°C resulted in a considerable decrease in the broad band region (3650-2750 cm^{-1}) for multicomponent glass powders especially for float glass (Figure 4.6c). After heat treatment at 600°C, the intensity of IR band at 3737cm^{-1}, attributed to isolated free Si-OH increased for all glass powders. In addition broad band (3650-2750 cm^{-1}) in the IR spectra of multicomponent glass powders disappeared after heating to 600°C (Figure 4.6d). For Fused silica on the other hand a small peak at 3650 cm^{-1}, corresponding to H-bonded OH groups (vicinal silanols) still remained on the surface of glass powders after heating at 650°C.

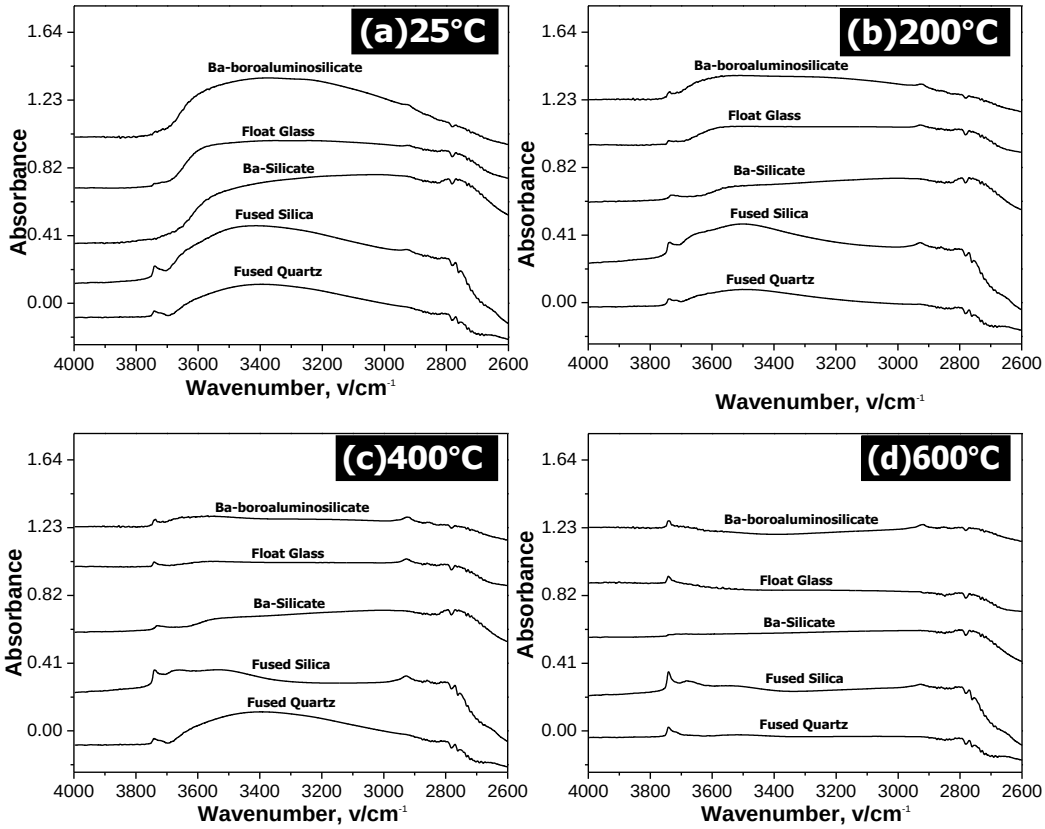

Figure 4.6 *The subtracted DRIFT spectra of glass powders (a) in as-prepared condition and after hating at (b) 200, (c) 400, and (d) 600°C*

Water Adsorption on Hydroxylated Glass Powders in situ DRIFT Spectroscopy

Water exposure experiments were conducted on as-prepared as well as heat treated glass powders at 150 and 600°C, via in situ DRIFT spectroscopy; the results are presented in Figure 4.7. The IR spectrum of KBr after exposure to 800µl of H_2O is shown on the bottom of all spectra in Figure 4.7, as a reference spectrum. The change in water adsorption bands located in the range of 3800-1650 cm^{-1} after exposure to water vapor was observed.

Figure 4.7a shows DRIFT spectra of as-prepared glass powders before and after exposure to 400 µl of H_2O. As shown in the Figure 4.7a, for float glass, Ba-silicate and fused quartz, there is no change in the intensity of IR band between 3800-2000 cm^{-1}, corresponding to physically adsorbed water and OH groups after exposure to 400 µl of H_2O. A small increase was detected in the intensity of the IR band between 3400-2800 cm^{-1} for Ba-boroaluminosilicate and fused silica. On the other hand, heat treatment of glass powders at 150°C enhances the adsorption of water on glass powders. As shown in Figure 4.7b, there is a considerable increase in the intensity of an IR band between 3400-2800 cm^{-1}, accompanied by a decrease in the intensity of a small IR band located at 3737 cm^{-1}, attributed to isolated Si-OH. The decrease in the intensity of IR band

between 3400-2800 cm^{-1} is highest in fused silica glass powders. H_2O started to adsorb on float glass, Ba-silicate and Fused Quartz after heat treatment at 150°C.

Figure 4.7c exhibits the IR spectra of heat treated glass powders at 600°C with distinct chemical compositions before and after exposure to 400µl of H_2O. Further heat treatment at 600°C does not lead to a big change in adsorption of water on fused quartz. IR bands located in the range of 3400-2800 cm^{-1}, attributed to physically adsorbed water, and at 3737 cm^{-1}, assigned to isolated Si-OH groups remained the same after exposure to 400µl of H_2O. On the other hand, for float glass and fused silica, the higher pretreatment temperature resulted in a significant increase in the IR band between 3400-2800 cm^{-1}, assigned to physically adsorbed water, accompanied by simultaneous decrease in the IR band at 3737cm^{-1}, attributed to isolated Si-OH groups. The Ba-silicate and Ba-boroaluminosilicate glasses, heat treated at 600°C, exhibit moderate increase in their IR bands related to physically adsorbed water. For all glass powders heat treated at distinct temperatures, no change was observed in the higher wavelength number region 3700-3600 cm^{-1} of broad IR band (3700-2600 cm^{-1}), attributed to molecular water.

4.3 Discussion

The infrared Spectroscopy (DRIFTs) as well as Thermogravimetric Mass Spectroscopy (TG-MS) results demonstrates that the degree of hydration on the glass surface is strongly dependent on the type and concentration of adsorption sites, which show great variation depending on the composition of the glass.

One of the significant structural differences which affect the degree of hydration is the presence of NBO. It is well known that non-bridging oxygen groups can act as primary surface sites for adsorption of water and have a tendency to form H bonding with OH groups [23]. The concentration of non-bridging oxygen groups differs depending on the chemical composition of glass. For fused silica and fused quartz, which do not contain non-bridging oxygen groups in their glass network, only weakly H-bonded Si-OH groups formed through charge compensation of unsatisfied Si^{4+} ions with atmospheric moisture, as evidenced by the IR band between 3650-3400 cm^{-1} (Figure 4.4a). These weakly H-bonded Si-OH groups are primarily responsible from further adsorption of water on silica surface in fused silica and fused quartz [38]. The degree of hydration on fused silica and fused quartz is limited to the concentration of H-bonded Si-OH groups due to lack of other available adsorption sites such as modifier ions or non-bridging oxygen.

On the other hand, multicomponent glasses such as Ba-silicate and float glasses have considerable amounts of Ba and Na modifier ions, resulting in formation of large number of non-bridging oxygen groups in the silicate network. These non-bridging groups can act as additional adsorption sites to enhance adsorption of water. The schematic description of NBO formation for different silicate glasses is shown in Figure 4.8. Basically, each Ba^{+2} and Na^{+} ion in Ba-silica

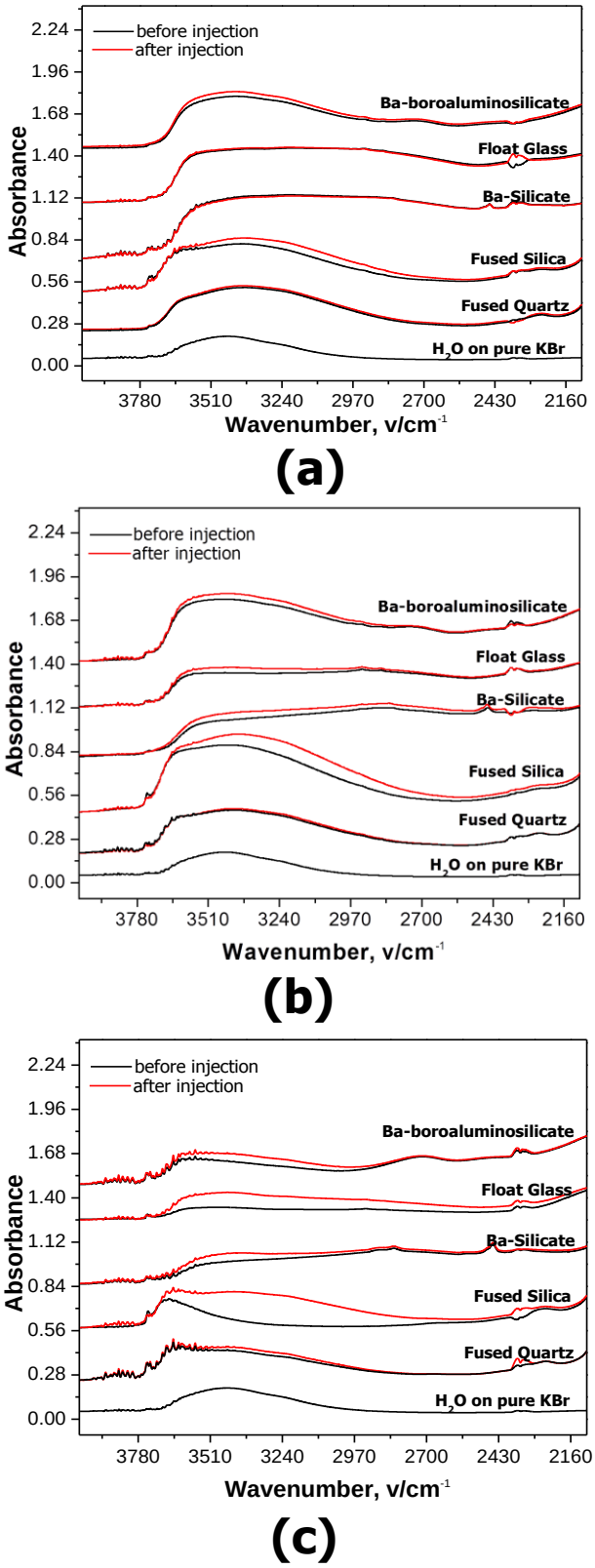

Figure 4.7 *DRIFT spectra of (a) as-prepared as well as pretreated glass powders at (b) 200 and (c) 600°C, before and after exposure to 400 µl H_2O*

and float glass generates two and one non-bridging oxygen groups, respectively to compensate for their charge in silicate network. The formation of non-bridging oxygen groups in Ba-silicate and float glass is confirmed by greater FWHM of the O(1s) spectra, suggesting a larger number of oxygen environments in these glasses and emergence of lower binding energy shoulder at 530.7 eV and 530.4 eV, respectively (Figure 4.1) [66]. These non-bridging oxygen groups, formed through introduction of alkaline (Na^{+}) or/and alkaline earth modifier (Ba^{2+}) ions into Ba-silicate and float glass, are very polarizable and thus can easily form very strong H-bonding with Si-OH groups on glass surface during reaction with atmospheric moisture, as evidenced by formation of IR band at 2700 cm^{-1} (Figure 4.4a) [37]. Meanwhile, unsaturated free modifier ions (Na^{+} or Ba^{2+}) can move to the glass surface and can interact with atmospheric moisture to form sodium or barium hydroxide groups on the glass surface. These hydroxide groups then react with carbon dioxide to form stable carbonate compounds such as $BaCO_3$ and Na_2CO_3 [67]. In our study, $BaCO_3$ formation was observed on Ba-silicate glasses whereas no evidence related to Na_2CO_3 formation on float glass surface was found. It has been thought that the higher field strength of barium ions, which enhances the concentration of negative charges on NBO groups, enhances carbonate formation on the Ba-silicate surface. The formation of $BaCO_3$ was confirmed by the emergence of characteristic $BaCO_3$ IR bands at 1750, 2452 and 2822 cm^{-1} (Figure 4.4c) [68] as well as the chemical shift of Ba($3d_{5/2}$) signal from 780.5 to 779.7 eV, which is close to the reported value for Ba($3d_{5/2}$) values of $BaCO_3$ (Figure 4.1) [69]. Formation of $BaCO_3$ on the Ba-silicate surface enhances the degree of hydration compared to float glass due to increased available adsorption sites, as evidenced by higher intensity of IR band between 3400-3200 as well as H_2O signal (m/z=18), attributed to physically adsorbed water on the glass surface.

In contrast to Ba-silicate and float glass, the structural arrangement of modifier ions which control the variety and concentration of available adsorption sites is completely different in Ba-boroaluminosilicate glasses. The Ba^{2+} ions in boroaluminosilicate glasses (1) provides charge compensation of $[AlO_4]^{-}$ tetrahedra species and (2) drive the boron atoms from three-fold coordination to four-fold coordination. This leads to an increase in network connectivity and prevents formation of non-bridging oxygen (Figure 4.8c) [70-71]. Based on the composition, NBO groups are not expected in this glass; i.e., all of the barium is consumed by charge compensation of the Al_2O_3 and B_2O_3. The absence of NBO groups in Ba-boroaluminosilicate glass is further confirmed through investigation of the high resolution O(1s) spectra (Figure 4.1). It is apparent that the FWHM of the O(1s) spectra of Ba-boroaluminosilicate is much smaller than that of Ba-silicate and float glass. Furthermore, the shoulder at 530.4 eV, attributed to non-bridging sites in glass, is not observable in the high resolution O(1s) spectra of Ba-boroaluminosilicate glass. This suggests that there are not any NBO groups in Ba-boroaluminosilicate glasses. The absence of non-bridging oxygen reduces the number of available adsorption sites on the glass surface. Moreover, the enhanced network connectivity in Ba-boroaluminosilicate glass likely eliminates significant bulk diffusion and also limits surface adsorption. This leads to a decrease in the amount of water adsorbed on glass. TG-MS spectroscopy results demonstrate that the number of H_2O per nm^2 in/on Ba-boroaluminosilicate

glasses is lower than the other multicomponent glasses like Ba-silicate and float glasses (Table 4.3).

The presence of additional adsorption sites, i.e. NBO in float glass and Ba-silicate and $BaCO_3$ on Ba-silicate glass makes the hydration of glass surface more favorable compared to fused silica and fused quartz. The number of H_2O per nm^2 is decreasing in the order of Ba-silicate, float glass, fused silica and fused quartz. The number of H_2O per nm^2 on Ba-silicate was found as 11.8, which is almost 4 times higher than that of fused quartz (Table 4.3).

The physically adsorbed water on different chemical composition glasses can be removed in the range of 50-200°C, as evidenced by a strong decrease in the intensity of IR band between 3400 and 3200 cm^{-1}, and emergence of H_2O signal (m/z=18) in MS spectrometer. In the dehydration process, first multiple layers of physically adsorbed water is removed between 25 and 150°C, then the H_2O monolayer is removed completely while the glass surface remains in a state of maximum hydroxylation. It has been found that the essential temperature range for loss of physically adsorbed water is strongly dependent on the chemical composition of glass. For fused silica and fused quartz the temperature range for desorption of physical water is between 50-125°C, whereas it is in the range of 50-200°C for multicomponent glasses such as Ba-silicate and float glass (Figure 4.2). The higher essential temperature for desorption of water from multicomponent glass is due to variation of adsorption sites. The three coordinated Si sites in the presence of NBO in/on multicomponent glasses will chemisorb water very strongly compared to [SiO_4] tetrahedra groups on fused silica and fused quartz [11-72]. The greater binding energy of water on coordination defects results in dehydration of water on multicomponent glasses at higher temperatures than that of silica counterparts.

Following the dehydration process, silanol (Si-OH) condensation, named as dehydroxylation, takes place at around 200°C by a decrease of the H-bonded vicinal pairs of OH groups condense to release water and increase the isolated Si-OH species (3737 cm^{-1}) [51, 61]. At temperatures above 400°C, most of the vicinal Si-OH groups condensed by thermal dissociation of hydrogen bonds, leading to a significant increase in concentration of free Si-OH groups (3737 cm^{-1}) [73]. The required temperature for condensation of H-bonded OH groups varies depending on the strength of the hydrogen bonds between OH groups and the glass network. For Ba-silicate and float glass, there are very strong H bonded Si-OH groups to NBO in addition to weakly H-bonded Si-OH groups. In contrast, fused silica and fused quartz surfaces contain only weakly H bonded Si-OH groups. During thermally induced dehydroxylation process, the weakest H bonds are the first to condense and then stronger H bonds (H bonded OH to NBO) condense at higher temperatures [74]. Thus, it is expected that the deydroxylation on fused silica and fused quartz takes place at lower temperatures compared to multicomponent glass (Figure 4.2).

After heat treatment at higher temperature around 600°C, isolated Si-OH groups still remained on the glass surface (Figure 4.4) because of the difficulty in interaction of the isolated Si-OH

groups with the other silanol groups [25]. Meanwhile, the IR band related to water or/and Si-OH groups (3600-3000 cm^{-1}) is still seen on fused silica and Ba-boroaluminosilicate glass after heat treatment at 600°C, suggesting that they are not on the glass surface; instead they occupy the interstices of glass network. D_2O exchange experiments showed that Ba-boroaluminosilicate and fused silica have a significant amount of structural water, mostly trapped as OH groups in the glass network (Figure 4.4) [23]. TG-MS results also support that fused silica and Ba-boroaluminosilicate have structural water as evidenced by the appearance of a H_2O signal in the range of 350-500°C (Figure 4.2). The presence of molecular water (1) affects the chemical state of water present on glass surface and (2) accelerates the degree of hydration on glass surface through formation of NBO and weakening of the glass network [43, 75]. In our study, fused silica exhibits a higher concentration of surface water as well as isolated silanol groups compared to fused quartz after all heat treatments (Figure 4.6). It is possible that molecular water, trapped mostly as OH groups, in the glass network alters the structure of glass through formation of H bonding with non-bridging oxygen. These H-bonded OH groups act as the main sites for further adsorption of water and thus enhance the hydration of water on fused silica. Furthermore, in-situ hydration experiment (Figure 4.7) supports that the presence of molecular water enhances the hydration rate of water on fused silica.

4.4 Conclusions

The differentiation of internal (structural) water in the glass network, from physically adsorbed water on the glass surface, was accomplished via in-situ D_2O exchange experiments. It has been found that the contribution of internal water to total water concentration is higher for fused silica and Ba-boroaluminosilicate glasses compared to that of their counterparts. Internal water in fused silica and Ba-boroaluminosilicate glass is mostly present as H bonded OH groups.

The type of water species on the glass surface was determined for glasses with different chemical compositions. Under environmental conditions, the presence of physically adsorbed water was confirmed for all glasses and could be almost completely removed after heating at 200°C. The degree of hydration (concentration of physically adsorbed water) can vary depending on type and concentration of H-bonded OH groups on glass surface which is strongly controlled by the amount of accessible adsorption sites on glass surface. The charge distribution at glass surface sites primarily determines the extent of water adsorption. In the case of Fused silica, Fused Quartz and Ba-boroaluminosilicate glasses, there is only weakly H bonded Si-OH groups for further adsorption of water (hydration) on the glass surface. On the other hand, Ba-silicate and Float glass surfaces have additional adsorption sites such as non-bridging oxygens which can form a strong H bonding with Si-OH groups due to their polarizability. Additionally, diffused Ba^{2+} ions to Ba-silicate glass surface generate Ba-OH groups which eventually react with CO_2 to form H_2O and $BaCO_3$ on the surface. The presence of non-bridging oxygen adsorption sites on

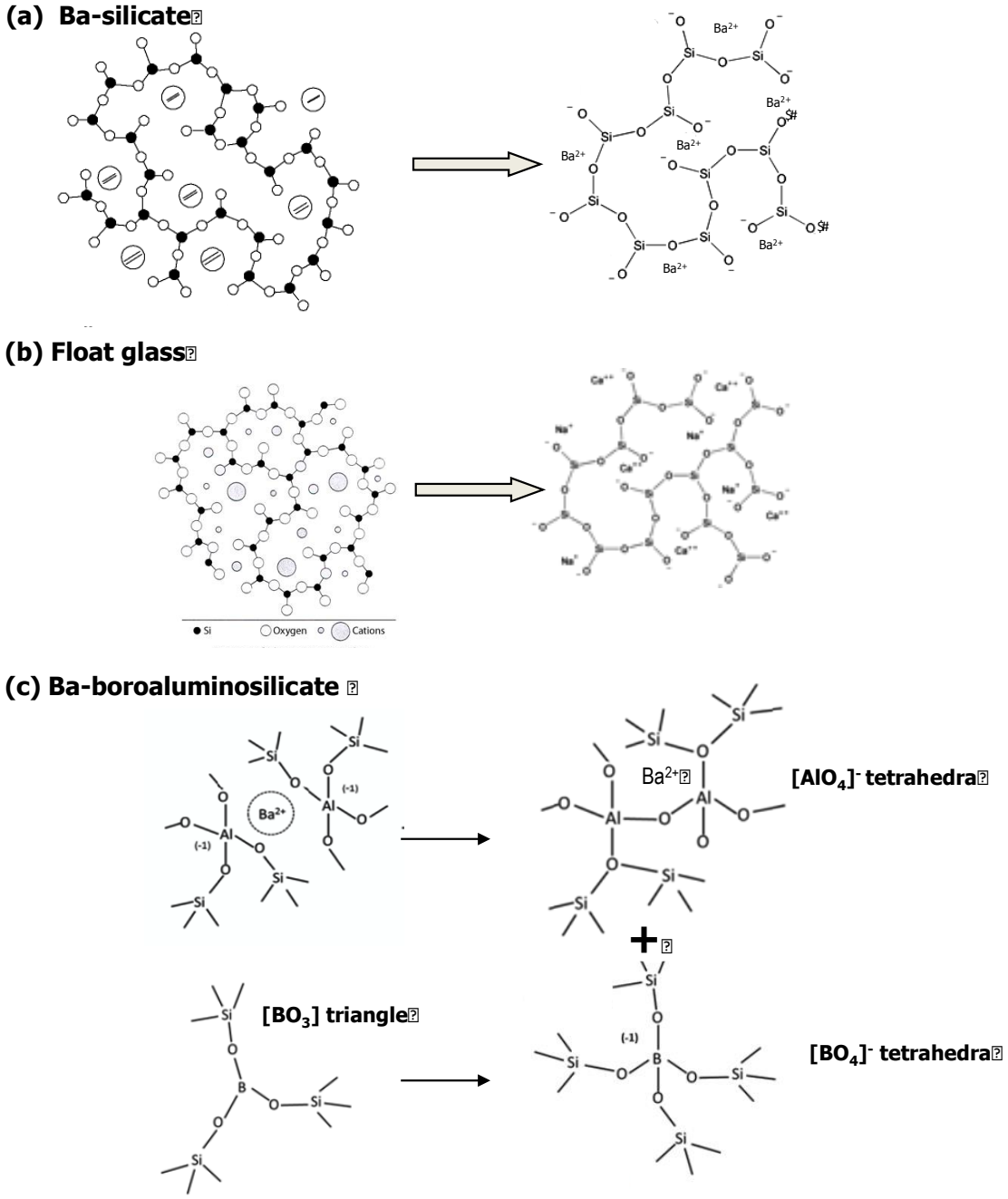

Figure 4.8 *Schematic representations of the (a) Ba-silicate, (b) float glass, and (c) Ba-boroaluminosilicate glass structures*

Float Glass and Ba-silicate glasses as well as $BaCO_3$ formation on Ba-silicate glass surface are responsible from their higher degree of hydration (Figure 4.9).

The concentration of H-bonded OH groups started to decrease after heat treatment at 200°C due to thermal dissociation of H-bonded OH groups to generate isolated Si-OH groups on the glass surface. The concentration of isolated Si-OH groups becomes higher with increasing heat treatment temperature to 650°C. For Ba-silicate, Ba-boroaluminosilicate and Float Glasses, all H-bonded Si-OH groups are diminished after heating at 650°C while a number of H-bonded Si-OH groups remained on fused silica and fused quartz surfaces.

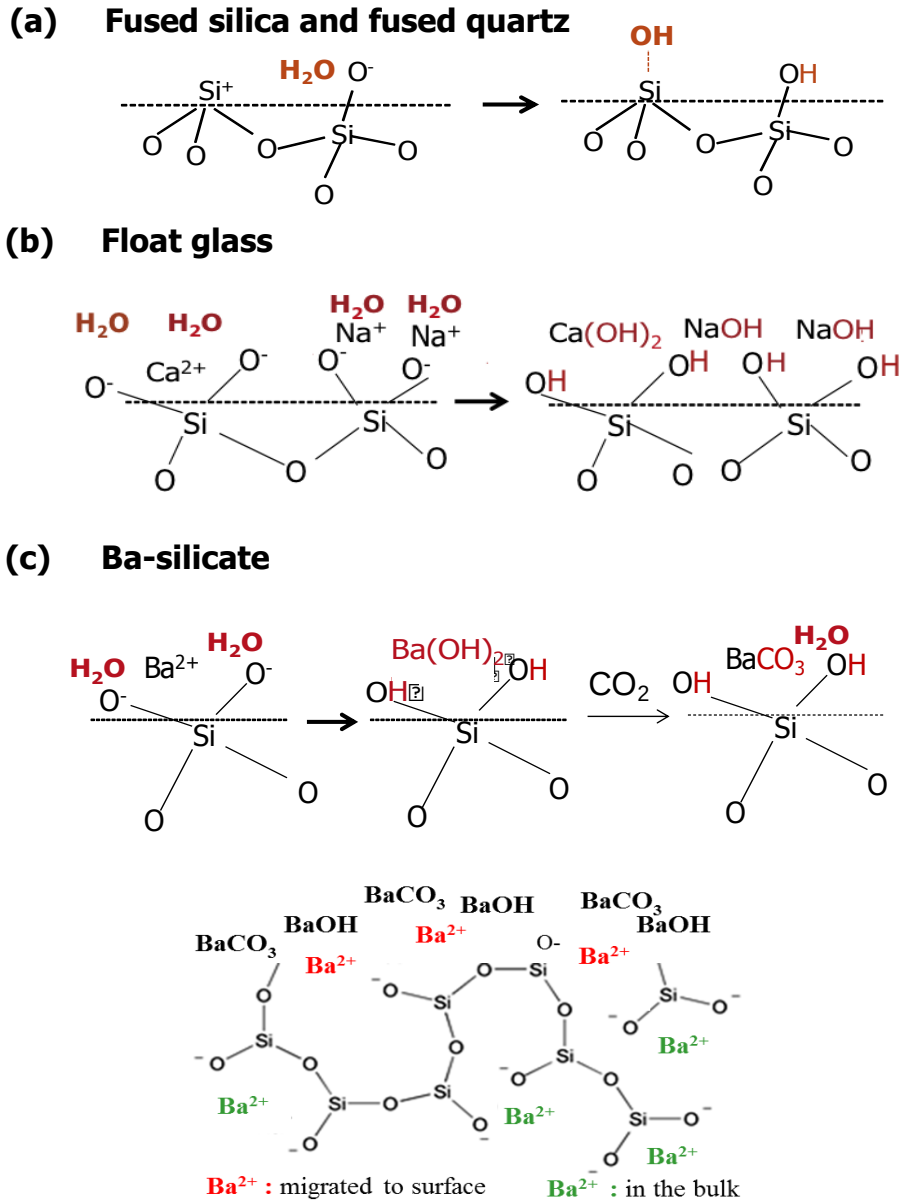

Figure 4.9 *Schematic representation of the type of water species on glass surfaces with different chemical compositions*

Chapter 5

WATER ADSORPTION on WET-GROUND GLASS POWDERS

5.1 Introduction

Adsorption on glass initiates whenever the surface is generated; either the melt surface (frozen liquid) on cooling or dry fracture surface post processing [11]. However, the extent of water adsorption depth is not limited to the outermost layer and is directly related to the concentration of modifier ions and environmental conditions while creating the new surface. For melt surfaces, the surface chemistry of glass is governed by the cooling rate. Moreover, the grinding media, ambient air and water significantly influence the variation of adsorption sites and degree of hydration on ground glass.

Multicomponent glass surfaces have a distribution of adsorption sites such as strained Si-O-Si bonds, coordination defects, free modifier ions and non-bridging oxygen ions, which are most likely to react with water moisture to form silanol groups on the surface. These silanol groups are responsible for further adsorption of water. The concentration of non-bridging oxygen is the predominant factor determining the degree and depth of hydration, as discussed in Chapter 4. When the number of NBO is high, an alkali depleted hydrated layer can form near the surface. However, the depth and degree of hydration decreases with increasing concentration of glass intermediates. The introduction of network intermediates, including B_2O_3 and Al_2O_3 decrease the number of non-bridging oxygen through conversion of $[BO_3]$ to $[BO_4]^-$ and charge compensation of $[AlO_4]^-$ sites [84]. The variety and concentration of adsorption sites on glass surfaces is also dependent on the way the surface is created. For example, wet-milling of glasses in liquid water may promote the formation of hydrated layer on glass surface by enhancing ion exchange process between modifier and H_3O^+ ions.

In this study, adsorption of water on wet-milled multicomponent glasses, i.e. Ba-silicate, and Ba-, Ca-, Mg- boroaluminosilicate glasses, was investigated. The variation in available surface adsorption sites on wet-milled glass powders as a function of chemical composition was determined by XPS and DRIFTs, and compared with dry-ground counterparts (in Chapter 4). The influence of prolonged wet milling time on surface chemistry of Ba-boroaluminosilicate glasses was studied by DRIFTs and TG-MS. The change in hydration temperature of Ba-boroaluminosilicate glasses as a function of wet-milling time is discussed. Furthermore, the effect of alkaline earth ions such as Ba^{2+}, Ca^{2+}, Mg^{2+}, on the structure of the boroaluminosilicate

network and adsorption sites was examined by XPS and DRIFTs. The concentration of water-related species in/on multicomponent glasses was determined by TG-MS spectroscopy.

5.2 Results

5.2.1 BET *(Brauner-Emmett-Teller)* Surface Area Analysis

Table 5.1 presents the surface area of glass powders in their as-prepared condition as well as after heat treatment at 650°C. Table 1a presents the surface area of multicomponent glass powders in their as-prepared condition and after heat treatment at 650°C. As shown in Table 5.1a, the surface area of Ba-silicate, Ca-boroaluminosilicate, Mg-boroaluminosilicate and Ba-boroaluminosilicate were found 6.5, 6.54, 6.94 and 5.54 m^2/g, respectively. They decreased to 6.24, 5.67, 5.81 and 5.16 m^2/g for Ba-silicate, Ca-boroaluminosilicate, Mg-boroaluminosilicate and Ba-boroaluminosilicate, respectively, after heat treatment to 650°C. These glasses can be considered as having approximately the same surface area.

Table 5.1 *BET surface area of (a) Ba-silicate, Ba-boroaluminosilicate, Ca-boroaluminosilicate, and Mg-boroaluminosilicate glass powders as well as (b) Ba-boroaluminosilicate powders with different particle sizes, before and after heat treatment at 650°C for 2h*

(a) Surface Area (m^2/g)	**25°C**	**650°C**
Ba-silicate	6.50±0.04	6.24 ±0.01
Ca-boroaluminosilicate	6.54±0.02	5.67±0.05
Mg-boroaluminosilicate	6.94±0.04	5.81±0.06
Ba-boroaluminosilicate	5.54±0.03	5.16±0.04

(b) *Surface Area (m^2/g)* **(Ba-boroaluminosilicate)**		
	25°C	**650°C**
0.4 µm	23.00±0.08	22.50±0.01
0.7 µm	12.91 ±0.06	11.87±0.06
1.0 µm	9.22±0.06	8.63±0.03
1.5 µm	5.54±0.05	5.16±0.02

Table 5.1b illustrates the surface area of Ba-boroaluminosilicate glasses with different particle size, in their as-prepared condition and after heat treatment at 650°C. As expected, the increase in surface area is directly related to the particle size. Glasses with smaller particle size show higher surface area. The surface area of Ba-boroaluminosilicate glasses with 0.4, 0.7, 1.0 and 1.5µm was found as 23.00, 12.91, 9.22 and 5.54 m^2/g, respectively. As shown in the Table 5.1b, the Ba-boroaluminosilicate glass with 0.4 µm particle size has higher surface area compared to other Ba-boroaluminosilicate glasses with 0.7, 1 and 1.5 µm particle sizes. Heat treatment of glass powders at 650°C resulted in a small decrease in surface area of glass powders. After heat treatment at 650°C, the surface area of Ba-boroaluminosilicate glasses with 0.4, 0.7, 1.0 and 1.5µm changed to 22.5, 11.87, 8.93 and 5.16 m^2/g, respectively.

5.2.2 X-ray Photoelectron Spectroscopy (XPS) Analysis

High resolution XPS scans were conducted to determine the presence of elements like adventitious C, Si, O and Al, B, Ba, Ca, Mg in some cases. Table 5.2 illustrates the atomic percentage of elements present in/on glass powders in as prepared condition as well as after thermal treatment at 650°C. The atomic percentage of modifier ions like Ba, Ca and Mg was found 9.4, 1, 2.9 and 4.1 for Ba-silicate, Ba-boroaluminosilicate, Ca-boroaluminosilicate and Mg-boroaluminosilicate glasses. The heat treatment at 650°C resulted in a slight decrease in the atomic percentage of modifier ions in glass powders except for Ba-silicate. The atomic percentage of Ba, Mg, Ca decreased to 0.9, 2.8, 3.5 respectively for Ba-boroaluminosilicate, Ca-boroaluminosilicate, Mg-boroaluminosilicate glasses, while it increased to 9.8 for Ba-silicate powders. There is also a small decrease in the atomic percentage of other constitutent such as O, Si, B and Al, present in glass powders after thermal treatment at 650°C.

Additionally, high resolution scans of modifier ions like Ba, Ca and Mg as well as O were performed to determine the chemical state of elements present in/on glass surface and the extent of connection in the glass network. Figure 5.1 exhibits the high resolution O(1s) and modifier ions like Ba(3d), Ca(3d) and Mg(2p) present in the glass powders. Figure 5.1a illustrates the high resolution Ba(3d), Ca(3d) and Mg(2p) regions of Ba-silicate, Ba-boroaluminosilicate, Ca-boroaluminosilicate and Mg-boroaluminosilicate glasses, respectively, in their as-prepared condition as well as after heat treatment at 650°C. The binding energy of Ba(3d) in Ba-silicate glass is 780.7 eV and it decreased to 780.2 eV after thermal treatment at 650°C. The position of Ba(3d) peak in Ba-boroaluminosilicate on the other hand was found as 780.9 eV and its position did not change after heating to 650°C. The binding energy of Ca(3d) doublet and Mg(2p) peak was found t be 351.73, 348.23 and 51.14 eV, respectively and their peak positions stay in the same binding energy range after heating to 650°C.

Figure 5.1b shows the high resolution O(1s) region for Ba-silicate, Ba-boroaluminosilicate, Ca-boroaluminosilicate and Mg-boroaluminosilictae glasses. As shown in Figure 5.1b, the binding energy of O(1s) peak was 532.17, 532.2 and 532.26 eV for Ca-boroaluminosilicate, Mg-boroaluminosilicate and Ba-boroaluminosilicate glasses, respectively. The full width at half-max (FWHM) of O(1s) are similar for these glass powders and did not change with heat treatment. The Ba-silicate glass powders on the other hand exhibits an increase in the full width at half-max (FWHM) of O(1s) peak, accompanied by appearance of a shoulder on the peak located at 531.05 eV in addition to main O(1s) peak at 532,17 eV. The binding energy change and appearance of a shoulder may indicate that there are different chemical environments for O atoms present in/on Ba-silicate glass powders.

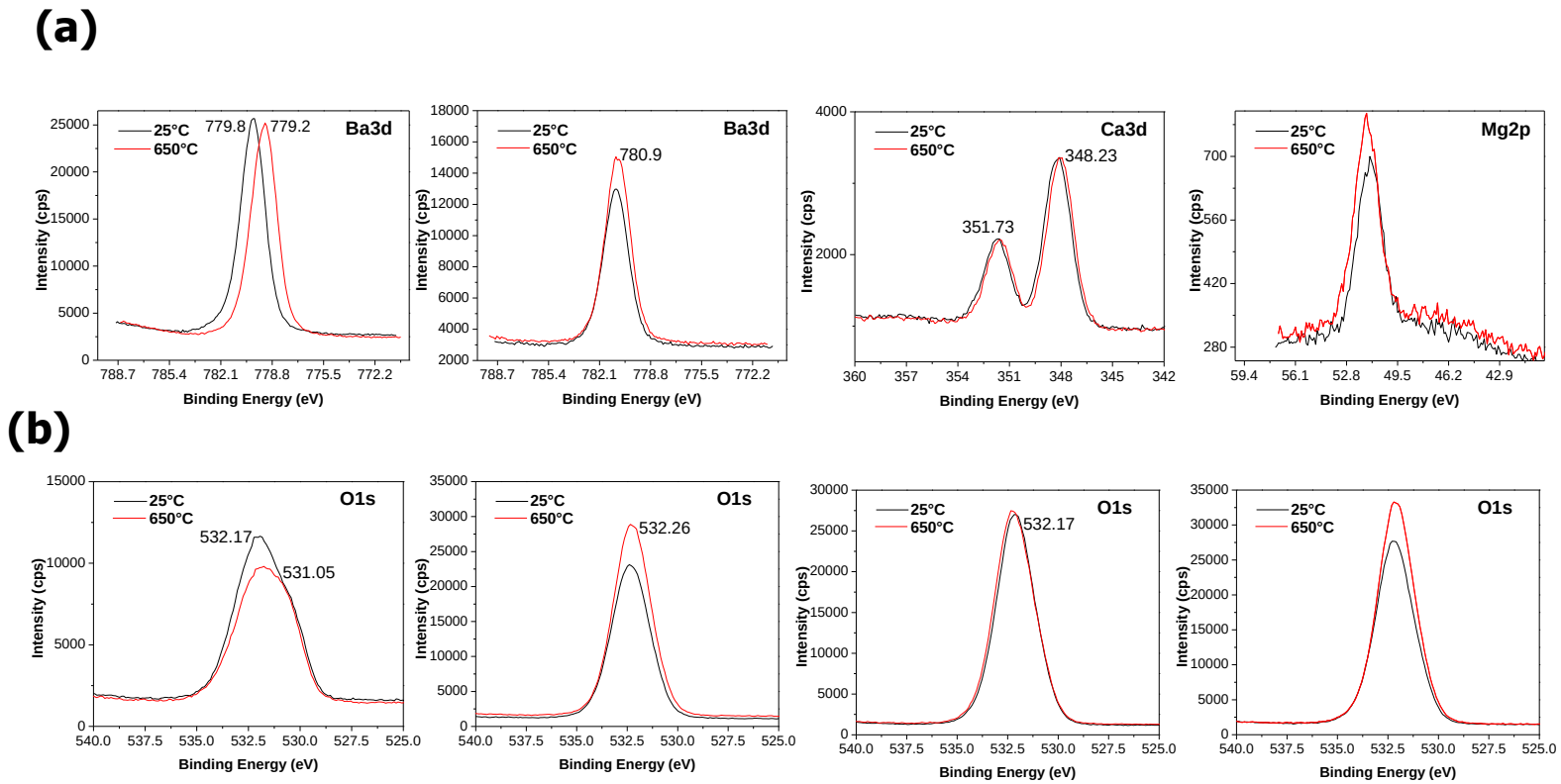

Figure 5.1 *High resolution (a) Ba 3d, Ca 3d, Mg 2p, and (b) O 1s spectra of Ba-silicate, Ba-boroaluminosilcate, Ca-boroaluminosilicate, and Mg-boroaluminosilicate glass powders in as-prepared condition as well as after heat treatment at 650°C*

.

Table 5.2 *Approximate chemical composition of the Ba-silicate, Ba-boroaluminosilicate, Ca-boroaluminosilicate, Mg-boroaluminosilicate glass powders before and after heat treatment at 650°C for 2h as determined by XPS*

25°C	**O (at.%)**		**Ca(at.%)**		**Mg (at.%)**		**B(at.%)**		**Si (at.%)**		**Al(at.%)**		**Ba(at.%)**	
	surface	*bulk*	*surface*	*bulk*	*Surface*	*bulk*	*surface*	*bulk*	*surface*	*bulk*	*surface*	*bulk*	*surface*	*bulk*
Ba-silicate	66.8	62.6							23.8	25			9.4	12.5
Ca-boroaluminosilicate	59	63	2.9	3.6			6	9	25.6	18.9	6.5	5.4		
Mg-boroaluminosilicate	59.7	63			4.1	3.6	6	9	25	18.9	6.4	5.4		
Ba-boroaluminosilicate	61.1	63					9.2	9	23.8	18.9	4.9	5.4	1	3.6

650°C (surface)	**O (at.%)**	**Ca (at.%)**	**Mg (at.%)**	**B (at.%)**	**Si (at.%)**	**Al (at.%)**	**Ba (at.%)**
Ba-silicate	69.8				20.4		9.8
Ca-boroaluminosilicate	60.1	2.8		5.7	25.3	6.1	
Mg-boroaluminosilicate	59.1		3.5	5.8	22.5	6.1	
Ba-boroaluminosilicate	62.3			9.1	22.8	4.9	0.9

5.2.3 Diffusion Reflectance Infrared Spectroscopy (DRIFTs)

Dehydration and Dehydroxylation Studies

In situ high temperature DRIFTs analysis of wet-ground modified glass powders was performed under Ar flow to detect water-related IR bands simultaneously. The DRIFT spectra of glass powders were collected at 150°C after heating at 200, 400 and 600°C for 30 min. Figure 5.2 shows the DRIFT spectra of glass powders in as-prepared condition (25°C) as well as at the other measured temperatures. Figure 5.2a exhibits the DRIFT spectra of glass powders with different chemical compositions at 25°C. As shown in Figure 5.2a, as-prepared Ba-, Ca- and Mg-borosilicate glass powders exhibit only broad IR band between 3710 and 2760 cm^{-1}. The higher wavelength region of this broad band between 3600-3400 cm^{-1} is attributed to surface or internal water inside the silica network, whereas the lower wavelength region between 3400-3200 cm^{-1}, corresponded to physically adsorbed water [51]. The same broad IR band in Ba-silicate glasses is wider and it located between 3650-2500 cm^{-1} with two maxima at 3529 and 2825 cm^{-1}. As shown in the Figure 5.2a, the intensity of this broad band is highest in Ba-silicate glass powders. For all glass powders, there is no clear IR band at 3737cm^{-1}, due to OH stretching vibration of isolated free Si-OH groups [35] at 25°C.

Figure 5.2b exhibits the DRIFT spectra of multicomponent glass powders with distinct modifiers like Ba, Mg and Ca. The intensity of broad band with two discernible maxima at 3600 and 3400 cm^{-1} slightly decreases after heat treatment at 200°C for 30 min, accompanied by emergence of small IR band at 3737 cm^{-1}, attributed to OH stretching vibration of isolated free Si-OH groups. Meanwhile, the lower wavelength region (3400-2800 cm^{-1}) of broad IR band for Ba-, Ca- and Mg-borosilicate glass powders diminished after heat treatment at 200°C. In Ba-silicate glass, the IR band at 3737 cm^{-1} is not symmetrical and it has an extension centered at 3710 cm^{-1}. In addition, Ba-silicate glass powder presents two additional IR bands located at 1750 and 2452 cm^{-1}, corresponding to formation of $BaCO_3$.

Figure 5.2c depicts the DRIFT spectra of glass powders with different chemical composition after in situ heating at 400°C. The heat treatment at 400°C leads to further decrease in intensity of the broad band located between 3710 and 2760 cm^{-1} for Ba-, Ca- and Mg-boroaluminosilicate glass powders and between 3529 and 2825 cm^{-1} for Ba-silicate glass powders. As shown in Figure 5.2.c, for all glass powders, heat treatment at 400°C leads to the appearance of a more well-defined IR band at 3737 cm^{-1}, corresponding to isolated Si-OH groups on the glass surface, accompanied by a significant decrease in intensity of broad IR peak region between 2400 and 3600cm^{-1}. The decrease in the broad IR band is less notable in Ba-boraaluminosilicate glass powders compared to all other multicomponent glass powders, whereas it is more severe in Ba-silicate

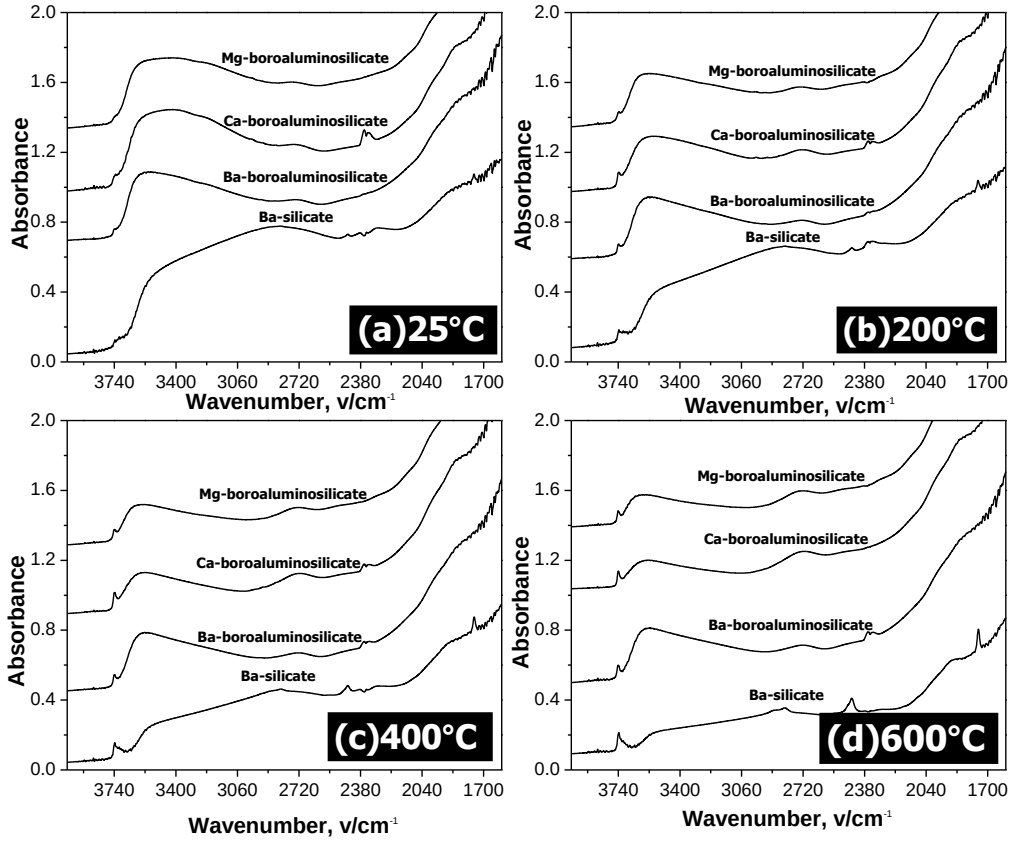

Figure 5.2 *DRIFT spectra of Ba-silicate, Ba-, Ca- and Mg-boroaluminosilicate glass powders (a) in as-prepared conditions and after heating at (b) 200, (c) 400, and (d) 600°C for 30 min.*

glass powders. Moreover, the intensity of IR band at 1750 and 2452 cm^{-1}, assigned to $BaCO_3$ formation in Ba-silicate glass, increases after heating to 400°C.

Figure 5.2d illustrates the DRIFT spectra of the glass powders, after in situ heat treatment at 600°C. For all samples, the intensity of IR band at 3737 cm^{-1}, assigned to free isolated Si-OH, increased. This IR band centered at 3737 cm^{-1} IR band in Ba-silicate is still not symmetrical and has an extension at 3710 cm^{-1}. There is a also simultaneous decrease in the intensity of broad IR band between 3710-2760 for Ba-, Ca-, Mg-boroaluminosilicate glasses and between 3529 and 2825 cm^{-1} for Ba-silicate glass powders. Meanwhile, heating to 650°C reveals additional IR band at 2822 cm^{-1}, attributed to $BaCO_3$ formation, in addition to 1750 and 2452 cm^{-1} in Ba-silicate glass powders. For Ba-boroaluminosilicate, the intensity of broad IR band between 3710-2760 cm^{-1}, corresponding to structural and physically adsorbed water is much higher compared to other glass powders.

Figure 5.2d indicates that water-related species remained on the glass surface after in situ heat treatment at 600°C for 30 min. Thus, external heat treatment at 800°C for prolonged time (8h) was conducted for all glass powders under Ar flow to determine the critical temperature for

dehydroxylation of glass. Figure 5.3 indicates the DRIFT spectra of the glass powders after external heat treatment at 800°C for 8h. As shown in Figure 5.3, even after this, there are still water-related IR bands in DRIFT spectra of the glass powders.

Figure 5.3a exhibits the DRIFT spectra of Ba-silicate glass powders. Heat treatment at 800°C resulted in disappearance of IR band at 3737 cm^{-1} (assigned to OH stretching vibration of isolated Si-OH groups) in Ba-silicate glass powders. Additionally, there is still a very broad weak IR band in the range of 3710 and 2529 cm^{-1}. Figure 5.3b shows the DRIFT spectra of Ba-boroaluminosilicate glass powders after heating at 800°C for 8h. As shown in Figure 5.3b, a broad IR band with two maxima at 3600 and 3200 cm^{-1} was detected. The intensity of this broad band is highest in the Ba-boroaluminosilicate glass powders. Figure 5.3c and Figure 5.3d illustrate the DRIFT spectra of Ca- and Mg-boroaluminosilicate glass powders, respectively, after heating at 800°C for 8h. DRIFT spectra of Ca- and Mg-boroaluminosilicate are very similar to that of Ba-boroaluminosilicate powders. No IR band related to OH stretching vibration of isolated Si-OH groups was observed. There is only a broad band with two maxima at 3600 and 3200 cm^{-1}.

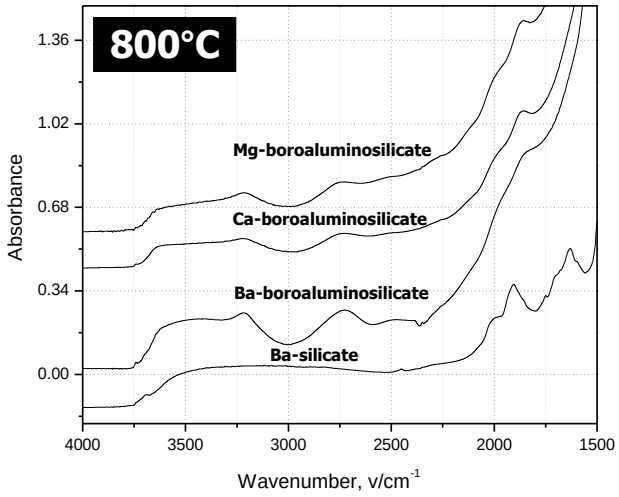

Figure 5.3 *DRIFT spectra of Ba-silicate, Ba-, Ca-, and Mg-boroaluminosilicate glass powders after heat treatment at 800°C for 8h*

DRIFT analysis was also performed on Ba-boroaluminosilicate glass powders as a function of particle size. Figure 5.4 shows the DRIFT spectra of Ba-boroaluminosilictae powders with different particle sizes of 0.4, 0.7, 1.0 and 1.5μm . Figure 5.4a exhibits the DRIFT spectra of Ba-boroaluminosilicate glasses with different particle sizes, after in situ heating at 50°C under Ar flow. The increase in particle size enhances the appearance of both IR band between 3710-2760 cm^{-1} and at 3737cm^{-1}, attributed to isolated Si-OH formation. As shown in the Figure 5.4a, very weak IR band at 3737 cm^{-1} appeared, accompanied by emergence of broad band between 3710-2760cm^{-1}, in Ba-boroaluminosilicate glass powders with 1.5μm particle size. However, the intensity of both IR band is enhanced with decrease in particle size of Ba-boroaluminosilicate powders. The intensity of a broad band between 3710-2760 cm^{-1} almost doubles with a decrease

in particle size of Ba-boroaluminosilicate glass powders from 1.5 to 0.4µm. Figure 5.4b presents the DRIFT spectra of Ba-boroaluminosilicate glass powders having different particle sizes, after heat treatment at 600°C. As shown in Figure 5.4b, the lower wavelength region, i.e 3200-2800 cm^{-1}, of a broad band, corresponding to physically adsorbed water, vanished after thermal treatment at 600°C and as a result the IR band centered at 3560 cm^{-1} became narrower. Meanwhile, the intensity of IR band at 3737 cm^{-1} increases after heating to 650°C. The increase in the IR band at 3737cm^{-1} became more defined with decrease in particle size of Ba-boroaluminosilicate powders as depicted in Figure 5.4b.

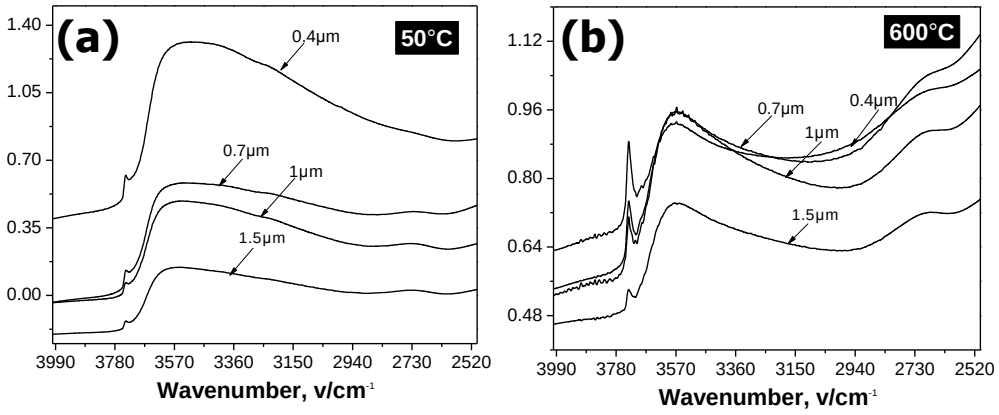

Figure 5.4 *DRIFT spectra of Ba-boroaluminosilicate glass powders with distinct particle size after heating at (a) 50, (b) 600°C for 30 min.*

The effect of grinding media on the degree of hydration was investigated by DRIFTs analysis of glass powder, prepared via wet-milling or dry-crushing. Figure 5.5 exhibits the DRIFT spectra of Ba-silicate and Ba-boroaluminosilicate powders, prepared by wet-milling or dry-crushing processes. As shown in Figure 5.5, both wet-ground Ba-silicate and Ba-boroaluminosilicate powders show higher intensity of IR band in the range of 3400-3200 cm^{-1} region, attributed to physically adsorbed water molecules.

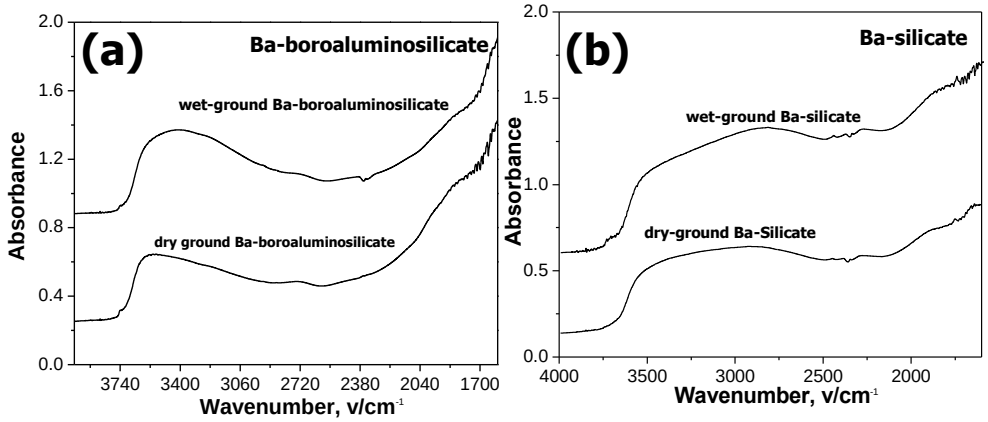

Figure 5.5 *DRIFT spectra of (a) Ba-boroaluminosilicate, (b) Ba-silicate powders after grounding in wet and dry media*

5.2.4 Thermogravimetric Mass Spectroscopy (TG-MS)

TG-MS analysis of glass powders with different chemical composition and particle sizes, were performed to obtain semi-quantitative information for released water-related species during heating. Figure 5.6 presents the TG-MS spectra of glasses with different chemical compositions. The spectra were obtained by collecting the change in sample weight and ionized product gases simultaneously during heating to 650°C at a rate of 10°C/min. As shown in Figure 5.6a, the decrease in sample weight of Ba-Silicate glass during heating is much more than all other glass powders. Because all these glass powders have similar surface area, as shown in Table 5.1, the mass change and the amount of released water species can be used to discuss the dehydration of glass powders. The mass change during heating to 650°C was found 3.34%, 1.03%, 0.80% and 0.74% for Ba-Silicate, Ba-boroaluminosilicate, Ca-boroaluminosilicate and Mg-boroaluminosilicate glass powders, respectively. The mass change in Ba-silicate glass powders is extremely high compared to other glass powders. MS spectra, presented in Figure 5.5b show similar results with TG spectra. Figure 5.6b exhibits the mass signals for released H_2O (m/z=18) gas for glasses with different chemical compositions. As shown in Figure 5.5b, the intensity of released H_2O (m/z=18) in Ba-silicate glass powders is much higher compared to other glass powders. The inset in Figure 5.6b shows the details of the mass signal attributed to H_2O for Ba-, Ca- and Mg-boroaluminosilicate glass powders. All glass powders except for Ba-boroaluminosilicate exhibit only one mass signal centered at 150°C for Ba-silicate and 180°C for Ca-, and Mg-boroaluminosilicate glass powders. This mass signal attributed to removal of physically adsorbed water. The H_2O signal in Ba-silicate glass powders is wider compared to that of other glass powders. As shown in inset in Figure 5.6b, the intensity of H_2O signal is decreasing in the order of Mg-, Ca-, Ba-silicate glass powders. Only Ba-boroaluminosilicate glass powders had an additional mass signal at 580°C, corresponding to removal molecular or internal water in silica network.

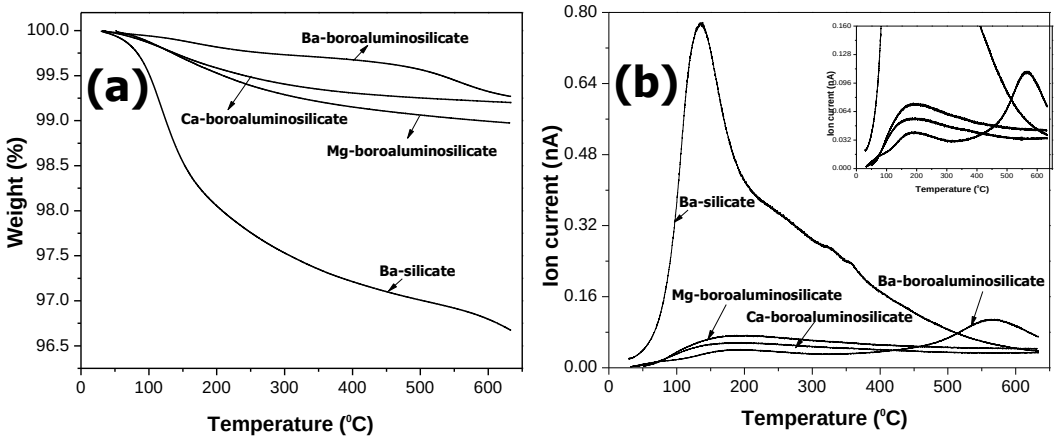

Figure 5.6 *(a) TG plots and (b) corresponding mass signals for evolved H_2O (m/z=18) for glass powders with different chemical compositions. The data were collected upon heating to 650°C*

Figure 5.7 exhibits the TG-MS spectra of Ba-boroaluminosilicate glass powders with different particle sizes, i.e 0.4, 0.7, 1.0 and 1.5µm. Figure 5.7a shows the mass change in glass powders during heating to 650°C. The percentage of mass decrease in Ba-boroaluminosilicate glass powders was found 2.6%, 1.27%, 0.8% and 0.7% for particle sizes of 0.4, 0.7, 1.0 and 1.5µm. As shown in Figure 5.7a, the total mass change during thermal treatment increased with a decrease in particle size for Ba-boroaluminosilicate powders. Figure 5.7b illustrates the mass signals attributed to evolved H_2O species during heat treatment at 650°C. Ba-boroaluminosilicate glass powders exhibit two distinct mass signals for removal of H_2O. The first mass signal emerged at 180°C and is attributed to removal of physically adsorbed water. The second mass signal appeared at 580°C and corresponded to internal water in the silicate network and as well as water inside the nanoporous structure near the glass surface. The decrease in particle size of Ba-boroaluminosilicate powders resulted in an increase in the intensity of all H_2O signals.

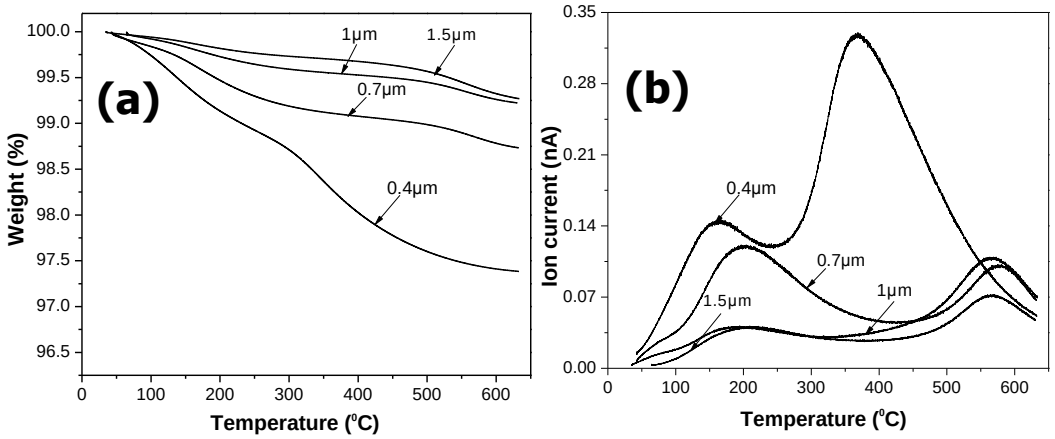

Figure 5.7 *(a) TG plots and (b) corresponding mass signals for evolved H_2O gas (m/z=18) for Ba-boroaluminosilicate glass powders with different particle size. The data were collected upon heating to 650°C*

Meanwhile, further decrease in particle size of Ba-boroaluminosilicate powders to 0.4µm, leads to emergence of mass signals, at lower temperatures. For Ba-boroaluminosilicate glass powders with 0.4µm particle size, H_2O mass signals appeared at 150°C and 400°C, attributed to physically adsorbed and internal water, respectively.

Figure 5.8 shows the mass signals attributed to evolved H_2O species, in wet- and dry-ground glass powders during heating to 650°C. Figure 5.8a illustrates that wet-ground Ba-boroaluminosilicate glass powders exhibit two distinct mass signals for removal of H_2O. The first mass signal emerged at 180°C and was attributed to removal of physically adsorbed water. The second mass signal with a higher intensity appeared at 580°C and corresponded to internal water as well as the water in porous structure near the surface. However, the intensity of mass signal appeared at 180°C decreases sharply while the second MS signal at 580°C disappeared for dry-ground Ba-boroaluminosilicate powders. The same trend was also observed for Ba-silicate

glasses. The wet-ground Ba-silicate glass powders exhibit higher and broader H_2O signal compared to dry-ground counterpart, as shown in Figure 5.8b.

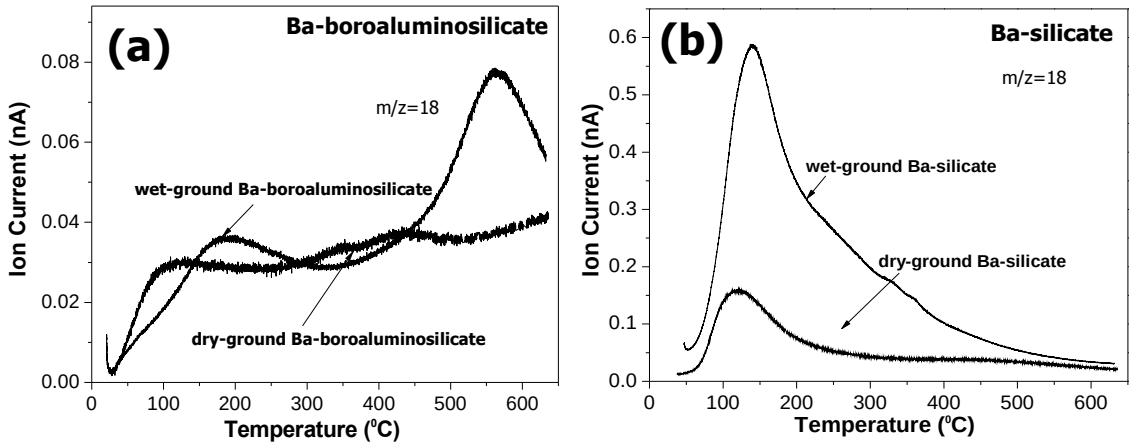

Figure 5.8 *MS spectra for evolved H_2O from (a) Ba-boroaluminosilicate and (b) Ba-silicate glass powders upon heating to 650°C*

Readsorption of Water on Dehydroxylated Glass Powders under Ambient Conditions

Rehydration of dehydroxylated glass powders was quantitatively evaluated by TG-MS spectroscopy as a function of time, i.e. 1 day, 1week and 1 month (Figure 5.9). The first and second run represents the TG-MS spectra of glass powders, collected upon sequential heat treatments to 650°C in TG furnace. Figure 5.9a presents the TG spectra of glass powders after heating to 650°C as well as after following exposure to ambient air for distinct times. As shown in Figure 5.9a, after second run, representing the second heat treatment to 650°C in TG furnace, no weight loss, attributed to water release, was observed for all glass powders. After exposure to ambient air, a gradual increase in percentage of water loss was detected for all glass powders. The percentage of water recovered in/on dehydroxylated glass powders during exposure to ambient air is highest in Ba-silicate glass powders. Figure 5.9b illustrates the MS signals for evolved H_2O gas during TG-MS analysis after exposure to ambient air for distinct times. As shown in Figure 4.6b, the MS signals, attributed to both physically adsorbed water and molecular water, disappeared after the second heat treatment at 650°C for all glass powders. After exposure to ambient air, only the MS signal, corresponding to physically adsorbed water started to reappear for all glass powders. The intensity of the mass signal for release of physically adsorbed water increased with exposure time. The amount of water readsobed during exposure to ambient air for 1 month is highest in Ba-silicate powders and it decreases in the order of Mg-, Ca-, Ba-boroaluminosilicate glass powders.

Quantitative analysis of glass powders after sequential thermal treatments at 650°C as well as after exposing to ambient air for distinct times were performed through integrating the area under mass signal for H_2O. Then the amount of water corresponding to integrated area under MS signal

for H_2O (m/z=18) was estimated from the calibration curve, shown in Figure 3.2. Then the amount of evolved H_2O was converted to the number of H_2O molecules per nm^2. Table 5.3 shows the number of H_2O molecules per nm^2 on/in glass powders during first and second heat treatment at 650°C as well as after exposure to ambient air for 1 day, 1 week and 1 month. The number of H_2O molecules per nm^2 was found 8.4, 35.4, 8.8 and 9.1 for Ba-boroaluminosilicate, Ba-silicate, Ca-boroaluminosilicate and Mg-boroaluminosilicate glass powders upon first heat treatment at 650°C. The number of H_2O molecules per nm^2 is very close to 0 upon the second heat treatment at 650°C. Exposure of glass powders to ambient air, on the other hand, resulted in an increase in the amount of water in/on glass powders. After 1 day exposure to ambient air, the number of H_2O molecules per $nm^2$was detected as 2.1, 8.2, 2.3 and 2.6 for Ba-boroaluminosilicate, Ba-silicate, Ca-boroaluminosilicate and Mg-boroaluminosilicate glass powders, respectively. The number of H_2O molecules per nm^2 increased to 3.2, 15.4, 3.1, and 3.6 after 1 week exposure to ambient air and finally, it reached to 4.8, 22.9, 4.5, and 5.2 for Ba-boroaluminosilicate, Ba-silicate, Ca-boroaluminosilicate and Mg-boroaluminosilicate glass powders, respectively after 1 month exposure to ambient air.

Table 5.3 *The number of water molecules released upon heat treatment of glass powders with distinct chemical compositions upon first and second heat treatment at 650°C as well as after exposure to atmos pheric moisture for 1 day, 1 week, and 1 month as determined by MS*

number of H_2O/nm^2	**1st run**	**2nd run**	**1 day**	**1 week**	**1 month**	**Surface area**
Ba-boroaluminosilicate	8.4	0.01	2.1	3.2	4.8	6.50 m²/g
Ba-silicate	35.4	0.02	8.2	15.4	22.9	6.54 m²/g
Ca-boroaluminosilicate	8.8	0.01	2.3	3.1	4.5	6.95m²/g
Mg-boroaluminosilicate	9.1	0.01	2.6	3.6	5.2	5.54 m²/g

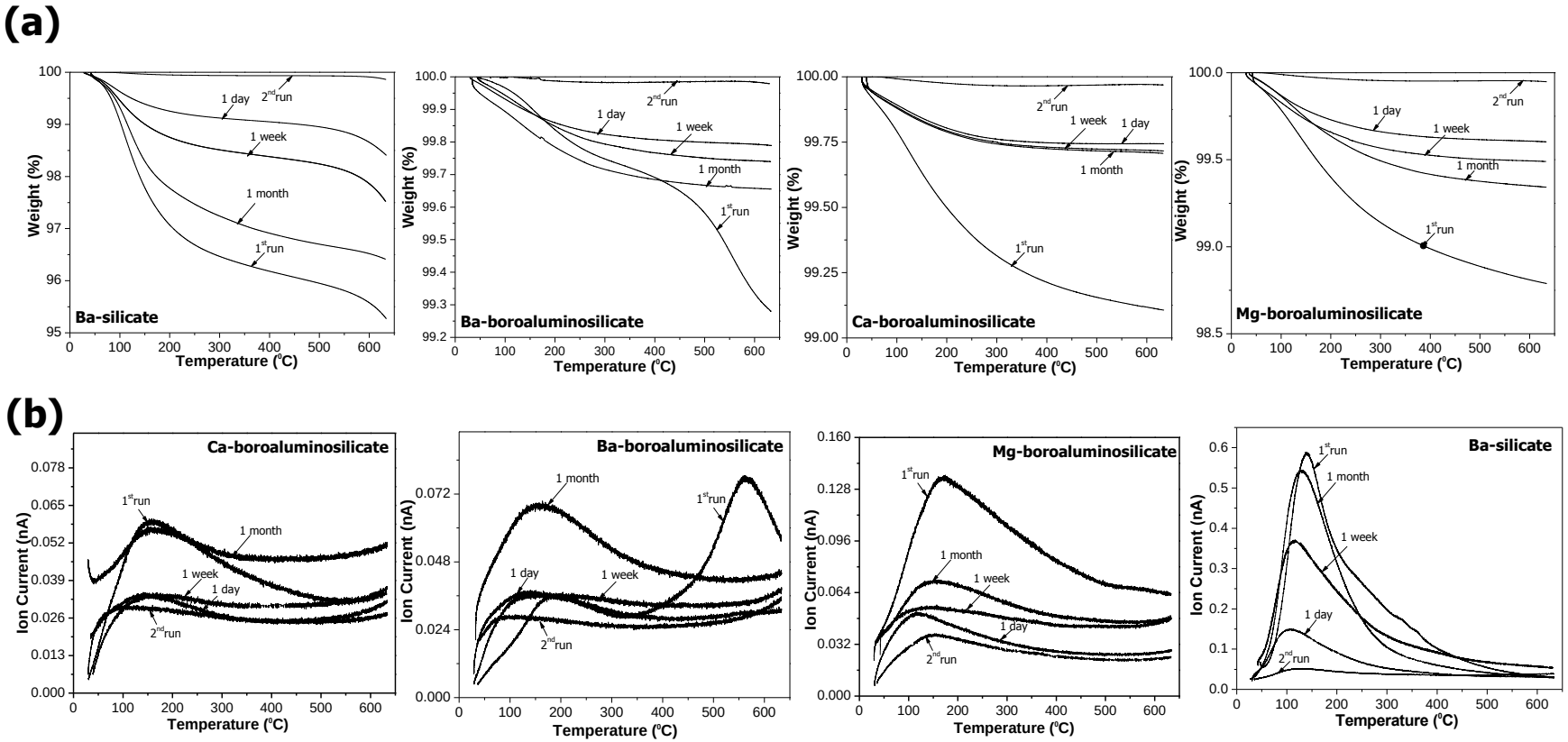

Figure 5.9 *(a) TG plots and (b) corresponding mass signals for evolved H_2O (m/z=18) for glass powders with different chemical compositions upon heating to 650°C (1st and 2nd run) as well as after exposure to atmospheric moisture for different times i.e. 1 day, 1 week and 1 month*

5.3 Discussion

The variety and concentration of available surface sites for adsorption of water is a function of both glass composition and particle size. Structural arrangement of modifier ions in the glass network glass, mainly governed by chemical composition of glass, is a key variable and controls the degree of hydration on the glass surface.

The most notable difference in structural arrangement of glass surface, which affects the degree of hydration, was observed between Ba-silicate and Ba-boroaluminosilicate glasses. In the case of Ba-silicate glasses, each Ba^{2+} creates two non-bridging oxygen ions (NBO) to compensate for the charge, as evidenced by the appearance of a lower binding energy shoulder on the high resolution O(1s) spectra at 530.4 eV (Figure 5.1) [66]. These non-bridging oxygen act as an active surface sites for adsorption of water and prone to form H bonding with surface OH groups, leading to emergence of an IR band at 2700 cm^{-1} (Figure 5-2) Additionally, free Ba^{2+} ions easily migrate to glass surface and then undergo ion-exchange of monovalent H^+ ions of environmental moisture to form barium hydroxide on the glass surface. These barium hydroxide groups readily react with carbon dioxide to form barium carbonate ($BaCO_3$) [67]. The formation of $BaCO_3$ was confirmed by the emergence of characteristic $BaCO_3$ IR bands at 1750, 2452 and 2822 cm^{-1} (Figure 5.2) [68] as well as the chemical shift of $Ba(3d_{5/2})$ signal from 780.6 to 779.8 eV, which is close to the reported value for $Ba(3d_{5/2})$ values of $BaCO_3$ (Figure 5.1) [69]. The chemical reactions resulting in formation of surface $BaCO_3$ are [76]:

$$\equiv SiO^- Ba^{2+} + H_2O \longrightarrow SiOH + BaOH \qquad \text{Eq. (5.1)}$$

$$Ba(OH)_2 + CO_2 \longrightarrow Ba(HCO_3)_2 \qquad \text{Eq. (5.2)}$$

$$Ba(OH)_2 + CO_2 \longrightarrow BaCO_3 + H_2O \qquad \text{Eq. (5.3)}$$

In contrast to Ba-silicate glasses, Ba-boroaluminosilicate glasses do not exhibit formation of either non-bridging oxygen or $BaCO_3$ which act as surface sites for adsorption of water. This is thought to arise from the presence of aluminum and boron species in the glass. In Ba-boroaluminosilicate glasses, alkaline earth ions (eg. Ba^{2+}) charge compensates boron and aluminum network species first and any excess will create non-bridging oxygen on silicon and boron network species. In our study, the amount of Ba is about 2.1% which is not enough to create non-bridging oxygen and free Ba^{2+} ions in the glass network. Thus, no evidence related to presence of non-bridging oxygen and $BaCO_3$ was found for Ba-boroaluminosilicate glasses. The charge compensation process of Ba^{2+} ions with boron and aluminum species increases the interconnectivity of glass structure, leading to a considerable decrease in available surface sites for adsorption of water.

The presence of additional adsorption sites like NBO and $BaCO_3$ makes the Ba-silicate glass surfaces more reactive toward water adsorption than Ba-boroaluminosilicate glass surfaces. The number of H_2O molecules per nm^2on Ba-silicate was found 35.4, which is approximately 3 times higher than that of their Ba-boroaluminosilicate counterparts. The relatively open network structure and variety of adsorption sites on Ba-silicate glasses also enhance (1) rehydration of glass surface under ambient atmosphere (Figure 5.7) and (2) dehydration of glass surface during in-situ heat treatment. The number of H_2O molecules per nm^2 on Ba-silicate glasses after rehydration under ambient conditions for 1month, reach to 22.9, which is close to its original value (35.4). On the other hand, dehydroxylated Ba-boroaluminosilicate glasses, which have more compact network structure, recover only part of the hydrated water during rehydration process under the same conditions. Furthermore, there is still considerable amount of water in/on Ba-boroaluminosilicate glasses after in-situ heat treatment at 650°C for 30 min., compared to Ba-silicate glasses (Figure 5.2).

Another effect of chemical composition on the degree of hydration was observed for boroaluminosilicate glasses having different modifier ions like Ba, Mg and Ca. Similar to alkaline modifier ions (Li, Na, K), the presence of alkaline earth ions in boroaluminosilicate glasses generates non-bridging oxygen in the glass structure. ^{17}O NMR studies in the literature showed that most of the non-bridging oxygen is associated with Si instead of B in boroaluminosilicate glasses [77]. The effect of alkali earth ions on structure of boroaluminosilicate glasses becomes predominant with decreasing modifier cation charge or increasing ion radius [36, 78-79]. Modifier ions with higher cation field strength (cation charge/size) in boroaluminosilicate glasses enhance the concentration of negative charges on non-bridging oxygen in their local coordination environment [77].

Besides the chemical composition, the particle size of glass powders also has a strong effect on hydration of glass surface. Both TG-MS and DRIFTs results clearly illustrate that the total water content of water in/on Ba-boroaluminosilicate glass increases with decrease in particle size (Figure 5.4 and Figure 5.6). This is most likely due to the effect of grinding medium (mainly water), on the structure of glass during the wet-milling process. Crushing of Ba-boroaluminosilicate glass powders in water initiates the ion exchange reaction between Ba^{2+} and H_3O^+ ions. The diffused Ba^{2+} ions leave a space in glass network and eventually a porous silicate layer formed near the glass surface. This makes the penetration of water into porous silicate structure easier during readsorption of water on glass surface. The degree of hydration of the glass surface increases for prolonged wet-milling process due to an increase in thickness of porous layer. In this study, Ba-boroaluminosilicate glass powders with 0.4μm particle size, exhibits the highest degree of hydration (Figure 5.4) due to prolonged wet-milling. The particle size of Ba-boroaluminosilicate glass powder also affects both dehydration and dehydroxylation temperatures. TG-MS results confirm that both dehydration and dehydroxylation of glass powders started at lower temperature as the particle size becomes smaller (Figure 5.6).

Moreover, a higher concentration of isolated silanols was found for Ba-boroaluminosilicate powders as the particle size becomes smaller, which is a sign of faster dehydroxylation.

The effect of wet grinding media, (mainly liquid water) on the surface structure of the glass and eventually the degree of hydration was also observed for Ba-silicate and Ba-boroaluminosilicate powders. Both the wet-ground Ba-silicate and Ba-boroaluminosilicate powders exhibits a higher degree of hydration compared to dry-ground counterparts, as evidenced by the higher intensity of the IR band between 3400-3200 cm^{-1} and the higher MS signal for evolved H_2O, attributed to physically adsorbed water (Figure 5.8 and Figure 5.9). It has been thought that the higher hydration degree of wet-ground Ba-boroaluminosilicate powders is due to the formation of nanoporous layer on the surface of glass, as a result of ion exchange process between Ba^{2+} and H_3O^+ ions. These nanoporous structure are more prone to the attack of water during wet milling and thus lead to greater hydration. The MS signal emerged at around 450°C in the Ba-boroaluminosilicate glass is believed due to evolved water coming from the porous layer upon heating. When the water inside the porous structure is removed, it did not come back upon exposure to atmospheric moisture even for 1 month (Figure 5.7).

5.4 Conclusions

The atomic structural arrangement of the glass surface which controls the concentration and variety of surface sites for adsorption of the water is strongly dependent on the chemical composition of glass. The variety and concentration of surface sites for adsorption of water in Ba-silicate glass greatly differ from Ba-boroaluminosilicate glasses. In Ba-silicate glass, each alkaline earth ion (Ba^{2+}) leads to formation of two non-bridging oxygens (NBO) and free Ba^{2+} ions on the glass surface first react with OH then CO_2 to form $BaCO_3$. In Ba-boroaluminosilicate glasses, on the other hand, the alkaline earth ions (Ba^{2+}) compensate boron and aluminum species and thus prevent formation of NBO as well as $BaCO_3$, leading to an increase in interconnectivity of the silicate network. The degree of hydration on the Ba-silicate glasses was approximately three times higher than that of Ba-boroaluminosilicate glass surface due to the presence of additional adsorption sites like NBO and formation of a more open silicate network.

The field strength of alkaline earth ions also influences the degree of hydration on the glass surface. The degree of hydration becomes higher as the cation field strength of boroaluminosilicate increases. This occurs because compensation of three coordinated to four coordinated boron in boroaluminosilicate glass becomes less favorable. The amount of physically adsorbed water is slightly higher on Ca and Mg boroaluminosilicates which have relatively higher cation field strength compared to Ba-counterparts due to higher fraction of three coordinated boron atoms. Additionally, the particle size of glass powders also has a strong effect on the hydration of a glass su

SUMMARY

In this thesis, the variation in type and concentration of water adsorption sites as a function of chemical composition of silica and silicate glasses was evaluated. Two distinct methods; crushing (ambient air) and wet-milling processes (aqueous media), were used to obtain glass powders and the effect of grinding medium on concentration of surface adsorption sites and degree of hydration was determined. A fundamental understanding of the surface chemistry of silica and silicate glasses upon exposure to in-situ heat treatment in DRIFTs was also obtained. Moreover, the structural water, trapped in interstices of silicate network was differentiated from surface water by D_2O exchange experiment The Infrared Spectroscopy (DRIFTs) as well as Thermogravimetric Mass Spectroscopy (TG-MS) results demonstrates the degree of hydration on glass surface is strongly dependent on the underlying structure of glass surface; including (1) non-bridging oxygen, (2) network intermediates; Al_2O_3 and B_2O_3 and (3) water already trapped in the bulk structure of the glass. The type of water-related species on different glass surfaces was determined in the as-prepared condition and upon exposure to in-situ heat treatment in DRIFTs. The presence of physically adsorbed water was confirmed for all glasses; it was completely removed after heating at 200°C. The degree of hydration was found to vary depending on the type and concentration of H-bonded OH groups on the glass surface. This, in turn, is strongly controlled by chemical composition of glass surface. For Ba-silicate and float glasses, the degree of hydration was found three times as high as that of fused silica and fused quartz due to the presence of high number of non-bridging oxygen, as confirmed by XPS analysis. These non-bridging oxygen ions can react with water to form H bonded SiOH groups due to their high polarizability. Moreover, Ba^{2+} ions on the Ba-silicate glass surface generate Ba-OH groups which eventually react with CO_2 to form H_2O and $BaCO_3$ on the surface. The presence of non-bridging oxygen adsorption sites on Float Glass and Ba-silicate glasses as well as $BaCO_3$ formation on Ba-silicate glass surface are responsible from their higher degree of hydration.

In contrast to the modifier ions, the addition of network intermediates such as Al_2O_3 and B_2O_3 decrease the concentration of the silanol groups and thus hydration rate. In Ba-boroaluminosilicate glasses, the alkaline earth ions (Ba^{2+}) compensate 4 fold coordinated boron and $[AlO_4]^-$ tetrahedra species and thus prevent formation of NBO as well as $BaCO_3$, leading to an increase in the interconnectivity of silicate network. This results in a decrease in the degree of hydration. The degree of hydration on Ba-boroaluminosilicate glasses was approximately three times less than that of the Ba-silicate glass surface. The effect of B_2O_3 on the structural connectivity of alkaline earth-containing boroaluminosilicate glass decreases with increasing field strength of alkaline earth ions. As the cation field strength of boroaluminosilicate increases,

the charge compensation reaction between the modifier ion and three coordinated boron becomes less favorable. It was found that the degree of hydration is slightly higher on Ca and Mg boroaluminosilicates which have relatively higher cation field strength compared to Ba-counterparts due to a higher fraction of three coordinated boron atoms. Besides the effect of chemical composition, milling of glass powders in aqueous environment also promotes the degree of hydration. The effect of milling media is more predominant in Ba-silicate glasses with a large number of non-bridging oxygen sites exposed by the creation of surface on the ground powders.

REFERENCES

[1] Tomozawa, M. Fracture of glasses. *Annu. Rev. Mater. Sci* 26, 43-74 (1996)

[2] Zhuravlev, L.T. The surface chemistry of amorphous silica. Zhuravlev model. *Colloids Surf, A* 173, 1-38 (2000)

[3] Scholze, H. Chemical durability of glasses. *Glass Ind* 47 (1966) 546, 622 670

[4] Moriya, Y., and Nogami, M. Hydration of silicate glass in steam atmosphere. *J. Non-Cryst. Sol.* 38&39, 667-672 (1980)

[5] Pantano, C. G. Surface Chemistry in relation to the strength and fracture of silicate glasses, Chapter III in Strength of Inorganic Glass (Ed. Kurkjian, C. H.) 37-67 (Plenum Press,New York, NY, 1985)

[6] Lymaris, O. V. Understanding multicomponent oxide interfaces using inverse gas chromatography. *MS thesis.* The Pennsylvania State University (2011)

[7] Wely, W.A. Structural changes in the glass surface and their technical iumplications, Chapter IV in Some practical aspects of the surface chemistry of glass, 57 (1947)

[8] Brunauer, S. The adsorption of gases and vapors: Physical adsorption (Princeton Univeristy Press, Princeton, N.J., 1945)

[9] Huang, R.J., Demirel , T., and McGee, T.D. Adsorption of water vapor on E-glass. J.*Am. Cer.Soc.* 55, 399-405 (1972).

[10] Dinh, L. N., Balooch, M., and LeMay, J. D. H_2O outgassing properties of fumed and precipitated silica particles by temperature-programmed desorption. *J. Colloid and Interface Sci*. 230, 432-440 (2000).

[11] Leed, E. A., and Pantano, C. G. Computer modelling of water adsorption on silica and silicate glass fracture surfaces. *J.Non-Cryst. Sol.* 48, 325 (2003)

[12] Ito, S., and Tomozawa, M. Dynamic fatigue and water in glass . *J. Phys. Colloq.* 61, 823 (1982)

[13] Han, W. T., and Tomozawa, M. Effect of residual water in silica glass on static fatigue *J. Non-Cryst. Solids* 127, 97-104 (1991)

[14] Hetherington, G., and Jack, K.H. Water in vitreous silica. *Phys. Chem. Glasses* 3, 129-133 (1962)

[15] Wagstaff, F. E., Brown, S. D., and Cutler, I. B. Influence of H_2O and O_2 atmospheres on the crystallization of vitreous silica *Phys. Chem. Glasses* 5, 76-81 (1964)

[16] Ciccotti, M., George, M., Ranieri, V., Wondraczek, L. and Marlière, C. Dynamic condensation of water at crack tips in fused silica glass (2007).

[17] Anderson, J. H., and Parks, G. A. The electrical conductivity of silica gel in the presence of adsorbed water. *J. Phys. Chem* 72, 3662-3668 (1968)

[18] Continuad, M., Bonniau, P., and Bunsell, A. R., The effect of water absorption on the electrical properties of glass-fiber reinforced epoxy composite. *J. Mater. Sci*. 17, 867 (1982)

[19] Bernett, M. K., and Zisman, W. A. Effect of Adsorbed Water on Wetting Properties of Borosilicate Glass, Quartz, and Sapphire. *J. Colloid and Interface Sci.* 3, 413-423 (1969).

[20] Leko, V. K., Chistokolova, M. V., Prokhorenko, O. A., and Mazurin, O.V. Effect of composition and temperature on intensity of absorption bands of water in alkali-silicate glasses. *Fiz. Khim. Stekla* 23(3), 308-325 (1997)

[21] Hair, M. L., and Hert, W. Adsorption on hydroxylated silica surfaces. *J Phys. Chem.* 73, 4269 (1969)

[22] Ghiotti, G., Garrone, E., Moterra, C., and Boccuzzi, F. I. Infrared study of low temperature adsorption. 1. Carbon monoxide on aerosil. An interpretation of the hydrated silica spectrum. *J. Phys. Chem.* 83, 2863-69 (1979)

[23] Stolper, E. The speciation of water in silicate melts. *Geochim. Cosmochim. Acta* 46(12), 2609-2620 (1982)

[24] McDonald, R. S. Surface functionality of amorphous silica by infrared spectroscopy, *J. Phys. Chem.* 62, 1168 (1957)

[25] Iler, R.K. The surface chemistry of silica , Chapter VI in The chemistry of silica 622 (A wiley-interscience publication, New York, NY, 1978)

[26] Kratachvila, J., Salajka, Z., Kzada, A., Kadlc, Z., Soucek, J., and Gheorgiu, M. Determination of hydroxyl groups and free water on silica gel in the near infrared region. *J. Non-Cryst. Solids.* 116, 93 (1990)

[27] Ek, S., Roat, A., Peussa, M., and Niinisto, L. Determination of hydroxyl group content in silica by thermogravimetry and comparison with H-1 MAS NMR results. *Thermochim. Acta* 379, 201-212 (2001)

[28] Agzamkhodzhaev, A. A., Zhuravlev, L. T., Kiselev, A. V., and Shengelya, K. Y. *Kolloidn. Zh.* 36, 1145 (1974)

[28] Gallas, J., Goupil, J. M., Vimont, A., Jean-Cloude., Gil, L. B., Gilson, J., and Miserque, O. Quantification of water and silanol species on various silicas by coupling IR spectroscopy and in-situ thermogravimetry. *Langmuir* 25(10), 5825 (2009)

[29] Davydov, V.Y., Kiselev, A.V., Zhuravle, L.T., Study of surface and bulk hydroxyl groups of silica by Infrared spectra and D_2O-exchange. *Langmuir* 60, 2254 (1964)

[30] McFarian, A. J. and Morrow, B. A. Infrared evidence for two isolated silanol species on activated silica. *J. Phys. Chem.* 14, 95 (1991)

[31] Morrow, B. A., and McFarlan, A. J. Chemical reactions at silica surfaces. *J. Non-Cryst. Sol*.120, 61-71 (1990)

[32] Smith, R. C ., and Kellum, G. E. Rapid condensation procedure for determination of hydroxyl in silicone materials. *Anal Chem.* 38, 67 (1966)

[33] Smith, R. C ., and Kellum, G. E. Determination of water, silanol, and strained siloxane on silica surfaces. *Anal. Chem*. 39, 341 (1967)

[34] Akinc Effect of drawing atmosphere on surface characteristic of glass fiber, Dissertation, Iowa State University (1977)

[35] Doremus, R. H. Infrared spectroscopy of glasses containing alkali ions. *J. Non-Cryst. Sol*. 41, 145-149 (1980)

[36] Bunker, B. C., Kirkpatrick, R. J., Brow, R. K., Turner, G. L., and Nelson, C. Local structure of alkaline-earth boroaluminate crystals and glasses: II, 11B and 27Al MAS NMR spectroscopy of alkaline-earth boroaluminate glasses. *J. Am. Ceram. Soc.* 74(6), 1430-1438 (1991)

[37] Wu, C-K. Stable silicate glasses containing up to 10 percent of water. *J. Non-Cryst. Sol*. 41, 381-398 (1980)

[38] Efimov, A. M., Pogareva, V. G., and Shashkin, A. V. Water-related bands in IR adsorption spectra of silica glasses. *J. Non-Cryst. Sol*. 332, 93-114 (2003)

[39] Ernsberger, F. M. Molecular water in glass. *J.Am. Cer. Soc*. 60, 91-92 (1977)

[40] Scholze, H. Glass-water interactions. *J. Non-Cryst. Sol*. 102, 1-10 (1988)

[41] Stevenson, C. M., and Novak, S. W. Obsidian hydration dating by infrared spectroscopy: method and calibration. *J. Archeological Sci*. 38, 1716-1726 (2011)

[42] Silver, L., and Stolper, E. Water in albitic glasses. *J. Petrology* 30, 667-709 (1989)

[43] Acocella, J., Tomozowa, M., and Watson, E. B. The nature of dissolved water in sodium silicate glasses and its effect on various properties. *J. Non-Cryst. Sol*. 65, 355-372 (1984)

[43] Silver, L., Ihinger, P. D., and Stolper, E. (1990). The influence of bulk composition on the speciation of water in silicate glasses. *Contrib Mineral Petrol* 104, 142-162, (1990)

[44] Navarra, G., Iliopoulos, I., Militello, V., and Leone, M. OH-realted infrared adsorption bands in oxide glasses. *J. Non-Cryst. Sol*. 351, 1796-1800 (2005)

[45] Stolper, E. Water in silicate glasses: An infrared spectroscopic study. *Contrib Mineral Petrol* 81, 1-17 (1982)

[46] Mysen, B. O. Interaction of water and melt in the system $CaAl_2O_4$-SiO_2-H_2O. *Chem. Geol*. 88, 223-243 (1990)

[47] Pandya, N., Muenow, D. W., Sharma, S. K., and Sherriff, B. L. The speciation of water in hydrated alkali silicate glasses. *J. Non-Cryst. Sol*. 176, 140-146 (1994)

[48] McMillan, P. F., and Remmele, R. L. Hydroxyl sites in SiO_2 glass: A note on infrared and raman spectra. *Am. Min*. 71, 772-778 (1986)

[49] Arai, E., and Terunuma, Y. Water adsorption in chemically vapor-deposited borosilicate glass film. *J. Electrochem. Soc*. 121, 676-681 (1974)

[50] DeRosa, R. L., Schader, P. A., and Shelby, J. E. Hydrophilic nature of silicate glass surfaces as a function of exposure condition. *J. Non-Cryst. Sol*. 331, 32-40 (2003)

[51] Uchino, T., Sakka, T., and Iwasaki, M. Interpretation of hydrated states of sodium silicate glasses by infrared and raman analysis. *J. Am. Cer. Soc*. 74., 306-313 (1991)

[52] Novak, S.W. Obsidian hydration dating by infrared spectroscopy: method and calibration. *J. Archeological Sci*. 38, 1716-1726 (2011)

[53] Zarubin, D.P. Infrared spectra of hydrogen bonded hydroxyl groups in silicate glasses: A re-interpretation. *Phys. Chem*. 40, 184-192 (1999)

[54] Wolters, D.R., and Verweij, H. Incorporation of water in silicate glasses. *Phys. Chem. Glasses* 22, 55-61 (1981)

[55] Kubicki, J. D., Sykes, D., and Rossman, G. R. Calculated trends of OH infrared stretching vibrations with composition and structure in aluminosilicate melts. *Phys. Chem. Minerals* 20, 425-432 (1993)

[56] Low, M. J. D., Ramasubramanian, N. Infrared study of the nature of the hydroxyl groups on the surface of porous glass. *J Physical Chem*.70, 2740-2746 (1965)

[57] Newman, S. S., Epstein, S., and Stolper, E. M. Measurement of rhyolitic glasses: calibration of an infrared spectroscopic technique. *Am. Min*. 71, 1527-1541 (1986)

[58] Bartholomew, R. F., Butler, B. L., Hoover, H. L.,and Wu, C. K. Infraraed spectra of a water-containing glass, *J. Am. Cer. Soc*. 63, 481-485 (1980)

[59] Kohn, S. C., Dupree, R., and Smith, M. Proton environments and hydrogen bonding in hydrous silicate glasses from proton NMR. *Nature* 337, 539-54 (1989)

[60] Farnan, I., Kohn, S. C., and Dupree, R. A study of the structural role of water in hydrous silica glass using cross-polarisation magic angle spinning NMR. *Geochim. Cosmochim.* 51, 2869-2873 (1987)

[61] Davis, K. M., and Tomozowa, M. An infrared spectroscopic study of water-related species in silica glasses. *J. Non-Cryst. Sol*. 201, 177-198 (1996)

[62] Foldes, E., Szabo, Z., Janecska, A., Nagy, G., and Pukanszky, B. Quantitative analysis of functional groups in HDPE powder by DRIFT spectroscopy. *Macromol. Symp*. 202, 97-15 (2003)

[64] Xue, X. Water Speciation in hydrous silicate and aluminosilicate glasses: Direct evidence from 29Si-1H and 27Al-1H double resonance NMR. *Am. Min*. 94, 395-398 (2009)

[65] Morrow, B.A.,and McFarlan, A. J. Surface vibrational modes of silanol groups on silica. *J. Phys. Chem*. 96, 1395-1400 (1992)

[66] Nesbitt, H. W., Bancroft, G.M., Henderson, G. S., Ho, R., Dalby, K. N., Huang, Y., and Yan, Z. Bridging, non-bridging and free (O_2^-) oxygen in Na_2O-SiO_2 glasses: An X-ray Photoelectron Spectroscopic (XPS) and Nuclear Magnetic Resonance (NMR) study. *J Non-Cryst. Sol.* 357, 170–180 (2011)

[67] Cerruti, M, and Morterra, C. Carbonate Formation on Bioactive Glasses. *Langmuir* 20, 6382 (2004)

[68] Roedel, E., Urakawa, A., Kureti, S., and Baiker, A. On the local sensitivity of different IR techniques: Ba species relevant in NO_x storage-reduction. *Phys. Chem.* 10, 6190-6198 (2008)

[69] Moulder, J. F., Stickle, W. F., Sobol, P. E., and Bomben, K. D. Handbook of x-ray photoelectron spectroscopy (Eds. Chastain, J., and King, R. C. Jr.) (1992)

[71] Golubeva, O.Y., and Pavinich, V.F. IR spectroscopic study of water in the structure of binary alkali borate glasses. *Glass Phys. Chem.* 31, 155-161 (2005)

[72] Leed, E. A, Sofo, J. O, and Pantano, C. G. Electronic structure of physisorption and chemisorption on oxide glass surfaces. *Phys. Rev. B* 72, 155427 (2005).

[73] Davis K. M., Agarwal, A., Tomozawa, M., and Hirao, K. Quantitative Infrared spectroscopic measurement of hydroxyl concentrations in silica glass. *J. Non-Cryst. Sol*. 203, 27-36 (1996)

[74] Leko, V. K., Chistokolova, M. V., Prokhorenko, O. A.,and Mazurin, O. V. Influence of composition and temperature on the adsorption band intensity for water in alkali silicate glasses. *Glass Phys. Chem.* 23, 214-224 (1997)

[75] Friedman, I., and Long, W. Hydration rate of obsidian. *Science* 159, 347-352 (1976)

[76] Schaut, R.A., The effect of boron oxide on the composition, structure, and adsorptivity of glass surfaces, Dissertation, The Pennsylvania State University (2008)

[77] Jingshi Wu, Composition and temperature effects on aluminoborosilicate glass structure and properties, Dissertation, Stanford University (2011)

[78] Du, L. S. and Stebbins, J. F. Network connectivity in aluminoborosilicate glasses: A high-resolution ^{11}B, ^{27}Al and ^{17}O NMR study. *J. Non-Cryst. Sol.* 351(43-45), 3508-3520 (2005)

[79] Roderick, J. M., Holland, D., Howes, A. P. and Scales, C. R. Density-structure relations in mixed-alkali borosilicate glasses by 29Si and 11B MAS-NMR. *J. Non-Cryst. Sol.* 293, 746-751 (2001)

[80] Scholze, H. Glass nature, structure and properties (Springer-Verlag, New York, 1990) (translated by Michael J. Lakin, 3rd ed)

[81] Stuke, A., Behrens, H., Schmidt, B. C., and Dupree, R. H_2O speciation in float glass and soda lime silica glass. *Chem. Geol*. 229, 64-77 (2006)

[82] Maciejewski M., Baiker A., Quantitative calibration of mass spectrometric signals measured in coupled TA-MS system. *Thermochim. Acta*. 295, 95-105 (1997)

[83] Varshneya, A.K. Fundamentals of inorganic glasses. (Academic Press, Inc, San Diego, 1994)

[84] Shelby, J.E. Introduction to glass science and technology. The Royal Society of Chemistry, 2nd ed., Cambridge, 2005)